Calhoun: The NPS Institutional Archive

DSpace Repository

Theses and Dissertations | 1. Thesis and Dissertation Collection, all items

1956-07

An investigation into the growth of a boiling boundary layer in turbulent flow.

Dyer, John Calvin

Massachusetts Institute of Technology

http://hdl.handle.net/10945/24742

Downloaded from NPS Archive: Calhoun

Calhoun is the Naval Postgraduate School's public access digital repository for research materials and institutional publications created by the NPS community. Calhoun is named for Professor of Mathematics Guy K. Calhoun, NPS's first appointed -- and published -- scholarly author.

Dudley Knox Library / Naval Postgraduate School
411 Dyer Road / 1 University Circle
Monterey, California USA 93943

http://www.nps.edu/library

AN INVESTIGATION INTO THE GROWTH OF A BOILING BOUNDARY LAYER IN TURBULENT FLOW

John Calvin Dyer

AN INVESTIGATION INTO THE GROWTH OF A BOILING BOUNDARY LAYER IN TURBULENT FLOW

by

John Calvin Dyer

B.S., United States Naval Academy
(1947)

SUBMITTED IN PARTIAL FULFILLMENT

OF THE REQUIREMENTS FOR THE

DEGREE OF MASTER OF SCIENCE

IN NUCLEAR ENGINEERING

at the

MASSACHUSETTS INSTITUTE OF TECHNOLOGY
July 1956

D77

Library
U.S. Naval Postgraduate School
Monterey, California

AN INVESTIGATION INTO THE GROWTH OF A BOILING BOUNDARY LAYER IN TURBULENT FLOW

by

Lieutenant John Calvin Dyer, U.S.N.

Submitted to the Department of Chemical Engineering on 20 August 1956 in partial fulfillment of the requirements for the degree of Master of Science in Nuclear Engineering.

ABSTRACT

The thickness of the boiling, bubble, boundary layer in forced convection flow in rectangular geometry was measured by photographs. The test section had a rectangular cross section (1/2 inch x 1/4 inch) which consisted of two opposite, electrically heated, stainless steel walls and two glass walls. The ratio of heated strip length to the spacing between the strips was about sixty. The range of the variables investigated was: heat flux density 0 to 475,000 Btu/hr ft^2; test section flow velocity 0 to 5 ft/sec; pressure 0 to 56 psia, and liquid subcooling between 27°F and 108°F at the test section inlet.

The bubble boundary layer thickness was plotted against a parameter which expressed the calculated bulk subcooling of the liquid at the point where the bubble layer thickness was measured. The plots show quantitatively the behavior of the bubble layer under various conditions of subcooling, flow, and heat flux density. An attempt was made to include the conditions of nucleation of boiling as a unifying parameter for the layer growth. While a significant relationship was indicated, there is little experimental basis for the proper value of nucleation superheat necessary at the pressures investigated. In addition there are undoubtedly other nucleation variables which are significant. A generalized correlation of bubble layer growth was not achieved.

Thesis Supervisor: John A. Clark

Title: Assistant Professor of Mechanical Engineering

[illegible]

AN INVESTIGATION INTO THE SHAPE

OF A BOILING BOUNDARY LAYER IN

THERMAL FLOW

by

Lieutenant John Calvin Dyer, U.S.N.

Submitted to the Department of Chemical Engineering on 26 August 1938 in partial fulfillment of the requirements for the degree of Master of Science in Nuclear Engineering.

ABSTRACT

The thickness of the boiling, bubble, boundary layer in forced aqueous flow in rectangular geometry was measured by photographs. The test section had a rectangular cross section (1/8 inch x 1/4 inch) which consisted of two opposite, electrically heated, stainless steel walls and two glass walls. The ratio of heated strip length to the spacing between the strips was about sixty. The range of the variables investigated was: heat flux density 0 to 473,000 Btu/hr ft²; test section flow velocity 0 to 5 ft/sec; pressure 0 to 50 psia, and liquid subcooling between 27°F and 108°F at the test section inlet.

The bubble boundary layer thickness was plotted against a parameter which expressed the calculated bulk subcooling of the liquid at the point where the bubble layer thickness was measured. The plots show quantitatively the behavior of the bubble layer under various conditions of subcooling, flow, and heat flux density. An attempt was made to include the conditions of nucleation of boiling as a modifying parameter for the layer growth. While a significant relationship was indicated, there is little experimental basis for the proper value of nucleation superheat necessary at the pressures investigated. In addition there are undoubtedly other nucleation variables which are significant. A generalized correlation of bubble layer growth was not achieved.

Thesis Supervisor: John A. Clark

Title: Assistant Professor of Mechanical Engineering

TABLE OF CONTENTS

	Page
Abstract	i
Table of Contents	ii
List of Illustrations	iii
Acknowledgement	v
Introduction	1
Description of Apparatus	3
Experimental Procedure	13
Discussion of Results	18
List of Symbols	24
Tables of Experimental Data	25
Graphic Plots of Data	28
Bibliography	41

TABLE OF CONTENTS

Abstract	i
Table of Contents	ii
List of Illustrations	iii
Acknowledgments	v
Introduction	1
Description of Apparatus	7
Experimental Procedure	13
Discussion of Results	18
List of Symbols	24
Tables of Experimental Data	25
Graphic Plots of Data	29
Bibliography	44

LIST OF ILLUSTRATIONS

Figure	Page
1. Schematic Flow Diagram	4
2. Photograph of Apparatus	5
3. Diagram of Approach Section to Test Section	7
4. Diagram of Center Section of Test Section	8
5. Diagram of Electric Heating Circuit in Test Section	10
6. Photograph of Test Section (disassembled)	12
7. Photograph of Boiling: Q/A = 83,000 Btu/hr ft^2 and v = 1 ft/sec	15
8. Photograph of Boiling: Q/A = 166,000 Btu/hr ft^2 and v = 1 ft/sec	16
9. Photograph of Boiling: Q/A = 250,000 Btu/hr ft^2 and v = 1 ft/sec	17
10. Plot of Bubble Boundary Layer Thickness vs. "subcooling" for Q/A = 83,000 Btu/hr ft^2	29
11. Plot of Bubble Boundary Layer Thickness vs. "subcooling" for Q/A = 166,000 Btu/hr ft^2	30
12. Plot of Bubble Boundary Layer Thickness vs. "subcooling" for Q/A = 250,000 Btu/hr ft^2	31
13. Plot of Bubble Boundary Layer Thickness vs. "subcooling" for Q/A = 333,000 Btu/hr ft^2	32
14. Plot of Bubble Boundary Layer Thickness vs. "subcooling" for Q/A = 416,000 Btu/hr ft^2	33
15. Plot of Bubble Boundary Layer Thickness vs. "subcooling" for Q/A = 475,000 Btu/hr ft^2	34
16. Plot of Bubble Boundary Layer Thickness vs "subcooling" for v = 1 ft/sec	35
17. Plot of Bubble Boundary Layer Thickness vs. "subcooling" for v = 2 ft/sec	36

LIST OF ILLUSTRATIONS

Figure	Page
1. Schematic Flow Diagram	4
2. Photograph of Apparatus	5
3. Diagram of Approach Section in Test Section	7
4. Diagram of Center Section of Test Section	8
5. Diagram of Electric Heating Circuit in Test Section	10
6. Photograph of Test Section (disassembled)	12
7. Photograph of Boiling: Q/A = 83,000 Btu/hr ft^2 and v = 1 ft/sec	15
8. Photograph of Boiling: Q/A = 166,000 Btu/hr ft^2 and v = 1 ft/sec	16
9. Photograph of Boiling: Q/A = 250,000 Btu/hr ft^2 and v = 1 ft/sec	17
10. Plot of Bubble Boundary Layer Thickness vs. "Subcooling" for Q/A = 83,000 Btu/hr ft^2	29
11. Plot of Bubble Boundary Layer Thickness vs. "Subcooling" for Q/A = 166,000 Btu/hr ft^2	30
12. Plot of Bubble Boundary Layer Thickness vs. "Subcooling" for Q/A = 250,000 Btu/hr ft^2	31
13. Plot of Bubble Boundary Layer Thickness vs. "Subcooling" for Q/A = 333,000 Btu/hr ft^2	32
14. Plot of Bubble Boundary Layer Thickness vs. "Subcooling" for Q/A = 416,000 Btu/hr ft^2	33
15. Plot of Bubble Boundary Layer Thickness vs. "Subcooling" for Q/A = 475,000 Btu/hr ft^2	34
16. Plot of Bubble Boundary Layer Thickness vs. "Subcooling" for v = 1 ft/sec	35
17. Plot of Bubble Boundary Layer Thickness vs. "Subcooling" for v = 2 ft/sec	36

LIST OF ILLUSTRATIONS

Figure	Page
18. Plot of Bubble Boundary Layer Thickness vs. "subcooling" for v = 3 ft/sec	37
19. Plot of Bubble Boundary Layer Thickness vs. " subcooling" for v = 4 ft/sec.	38
20. Plot of Bubble Boundary Layer Thickness vs. "subcooling" for v = 5 ft/sec.	39
21. Plot of Bubble Boundary Layer Thickness vs. "subcooling and nucleation parameter"	40

LIST OF ILLUSTRATIONS

FIGURE	PAGE
18. Plot of single boundary layer thickness vs. "subsonic" for $\gamma = 1$ ft/sec	17
19. Plot of single boundary layer thickness vs. "subsonic" for $\gamma = 1$ ft/sec.	18
20. Plot of single boundary layer thickness vs. "subsonic" for $\gamma = 0$ ft/sec.	19
21. Plot of single boundary layer thickness vs. "subsonic and unstable particles"	20

Acknowledgment

The author is indebted to Professor John A. Clark for suggesting and supervising this investigation and to the Department of Mechanical Engineering of the Massachusetts Institute of Technology for the use of its research facilities.

He is grateful to the U.S. Naval Postgraduate School, Monterey, California for the necessary financial assistance.

He wishes to thank the craftsmen, particularly Robert Simpson, Herbert Norquist and William Liddy of the Central Tool Shop of the Boston Naval Shipyard for manufacturing the test section. Much credit is also given to Fred Johnson and Edward Hartell of the Heat Transfer Laboratory at the Massachusetts Institute of Technology for their ready assistance in the myriad details of assembling the test loop. In addition, the success of the photographic work was due to the skill and patience of Fred Johnson.

He also wishes to thank his wife, Glenys Dyer, who typed this thesis.

Acknowledgment

The author is indebted to Professor John A. Clark for suggesting and supervising this investigation and to the Department of Mechanical Engineering of the Massachusetts Institute of Technology for the use of its research facilities.

He is grateful to the U.S. Naval Postgraduate School, Monterey, California for the necessary financial assistance.

He wishes to thank the draftsman, particularly Robert Simpson, Herbert Morquist and William Liddy of the Central Tool Shop of the Boston Naval Shipyard for manufacturing the test section. Much credit is also given to Fred Johnson and Howard Bartell of the Heat Transfer Laboratory at the Massachusetts Institute of Technology for their ready assistance in the myriad details of assembling the test loop. In addition, the success of the photographic work was due to the skill and patience of Fred Johnson.

He also wishes to thank his wife, Glenys Dyer, who typed this thesis.

INTRODUCTION

The use of flat plate type fuel elements in nuclear reactors and the desire to achieve the higher heat transfer rates that are possible with the boiling process require more fundamental information on boiling under conditions of flat plate geometry. It was the objective of this investigation to make a photographic study of the boiling boundary layer growth under flow conditions using geometry and a ratio of coolant volume to heating surfaces which would more nearly approximate conditions in a nuclear reactor core. Previous investigations of pool boiling have generally used single heated wires or rods in a pool of water where the bubble size was large in relation to the heating surfaces, and the volume of fluid was much greater than the heating surface. The forced convection boiling has been done predominantly inside circular channels which is not the geometry of interest here.

Apparently the first work with rectangular flow channels was done by Gunther (1)* who had the heating strip in the center of the channel with water on both sides. As the intention was a study of bubble dynamics, rather than the growth of a bubble layer, the heated strips used by Gunther were not long. Argonne National

* Numbers in parentheses refer to the references in the bibliography.

INTRODUCTION

The use of flat plate type fuel elements in nuclear reactors and the desire to achieve the higher heat transfer rates that are possible with the boiling process require more fundamental information on boiling under conditions of flat plate geometry. It was the objective of this investigation to make a photographic study of the boiling boundary layer growth under flow conditions using geometry and a ratio of coolant volume to heating surfaces which would more nearly approximate conditions in a nuclear reactor core. Previous investigations of pool boiling have generally used single heated wires or rods in a pool of water where the bubble size was large in relation to the heating surfaces, and the volume of fluid was much greater than the heating surface. The forced convective boiling has been done predominantly inside circular channels which is not the geometry of interest here.

Apparently the first work with rectangular flow channels was done by Gunther (1)* who had the heating strip in the center of the channel with water on both sides. As the intention was a study of bubble dynamics, rather than the growth of a bubble layer, the heated strips used by Gunther were not long. Argonne National

* Numbers in parentheses refer to the references in the bibliography.

Laboratory has done extensive work with flat plate geometry in boiling conditions, but the only published information to date has been for natural convection (2). The writer was informed that work on boiling in forced convection in rectangular flow channels had been done at ANL, but no reports were available.

None of the foregoing published investigations used forced convection in flow geometry with oppositely facing heating elements having a large L/y, ratio of length to spacing between plates. The heat transfer section which was used consisted of two electrically heated flat, stainless steel (18-8) strips with degassed (de-aerated) distilled water flowing between them. L/y for this experiment was about 60. The range of the variables investigated was: heat flux density 0 to 475,000 Btu/hr ft^2; test section flow velocity 0 to 5 ft/sec; pressure at test section outlet 0 to 56 psia, and liquid subcooling between 27°F and 108°F at the test section inlet.

A description of the apparatus used, a discussion of the test procedure, and the test results are given in subsequent sections.

laboratory on zero gravity was also first given consent in orbital experiments, but the only published investigation to date has been the natural convection (1). The author and Ingersoll have work on cooling in forced convection in rectangular flow channels and have done at ARL, but no reports were available.

Lack of the formulation, sufficient investigations and forced convection in flow geometry with experiment result having elements varying a large L/r, yield or length to heating between plates. The best separate equation which was found consisted of two electrically heated flat, rectangular stand (10-7) series with expansion (low-speed). electrical wires trailing between them. L/r for this experiment was large ca. The range of the previous investigations was: heat flux density q is $\pm 17,000$ Btu/hr ft^2; free convection flow velocity 0 to 1 ft/sec; pressure at test section outlet 0 to 30 psia, and liquid properties, between ν/α and $10\nu/\alpha$ at the test section inlet.

A description of the experiment used, a discussion of the data procedure, and the test results are given in subsequent sections.

DESCRIPTION OF APPARATUS

The experimental equipment used to carry out this investigation is shown in the accompanying diagrams. Fig. 1 is a schematic flow diagram of the test loop. Fig. 2 is a photograph of the apparatus showing the test section in the vertical position. The pump and electrical preheaters are not visible in the photograph.

Distilled and degassified water was circulated in the test loop. This water was preheated before entering the test section by two electric heaters (Electric Chromelox immersion heaters, type WT 270, 7000 watts, 240 volts, E.L. Wiegand Co., Pittsburgh, Pa.). These heaters were controlled by Variacs, type V10G2, General Radio Co., Cambridge, Mass. A simple coiled tube heat exchanger using cold water was used to cool the water leaving the test section before entering the pump (Westinghouse totally enclosed centrifugal pump, model 30A, 220 volts, 3 phase, 60 cycle). This pump required an oil cooling system which had an oil to water cooled heat exchanger (Rose Heater and Manufacturing Co., Buffalo, N.Y.) and an electrically driven centrifugal pump, 10 gpm, Allis Chalmers Manufacturing Co., Norwood, Ohio. The motor for the oil pump was 3/4 HP, 440 volt, 60 cycle, 3 phase, General Electric. The water circulating pump discharged to a 3/4 inch square edged orifice for flow

DESCRIPTION OF APPARATUS

The experimental equipment used to carry out this investigation is shown in the accompanying diagrams. Fig. 1 is a schematic flow diagram of the test loop. Fig. 2 is a photograph of the apparatus showing the test section in the vertical position. The pump and electrical preheaters are not visible in the photograph.

Distilled and deaerated water was circulated in the test loop. This water was preheated before entering the test section by two electric heaters (Electric Capacitor Annealing Heaters, type WT 275, 7000 watts, 240 volts, Ill. Diamond Co., Pittsburgh, Pa.). These heaters were controlled by Variacs, type 3100, General Radio Co., Cambridge, Mass. A simple coiled tube heat exchanger using cold water was used to cool the water leaving the test section before entering the pump (Westinghouse totally sealed centrifugal pump, model 2VC, 220 volts, 3 phase, 60 cycle). This pump employed an oil cooling system which has an oil to water cooling heat exchanger (Lone Heater and Manufacturing Co., Buffalo, N.Y.) and an electrically driven centrifugal pump (Lone Ellis Chalmers Manufacturing Co., Norwood, Ohio). The motor for the oil pump was 3/4 HP, 440 volt, 60 cycle, 3 phase, Reactor Electric. The water circulating pump discharged to a 3/4 inch square edged orifice for flow

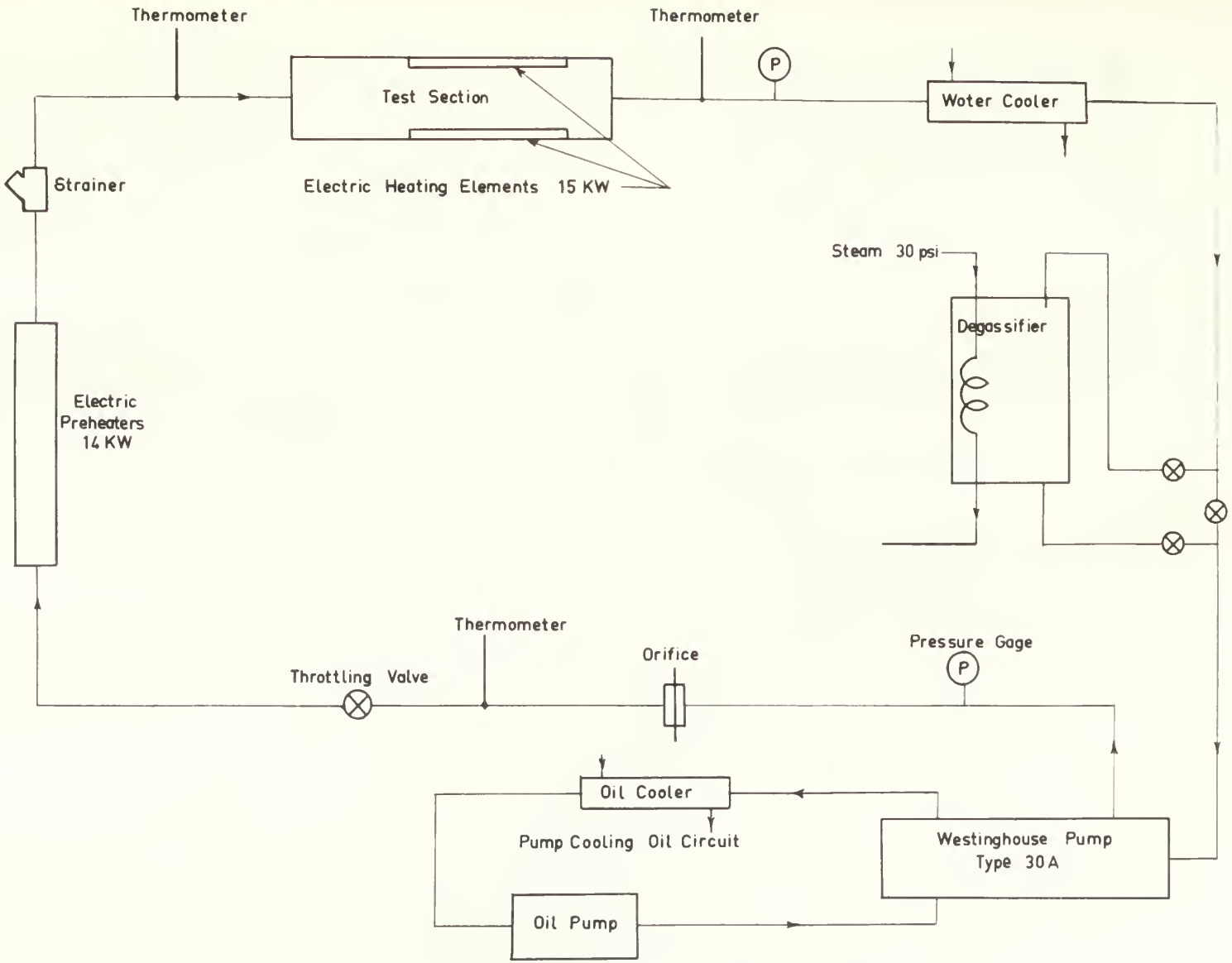

Fig. 1 - SCHEMATIC FLOW DIAGRAM

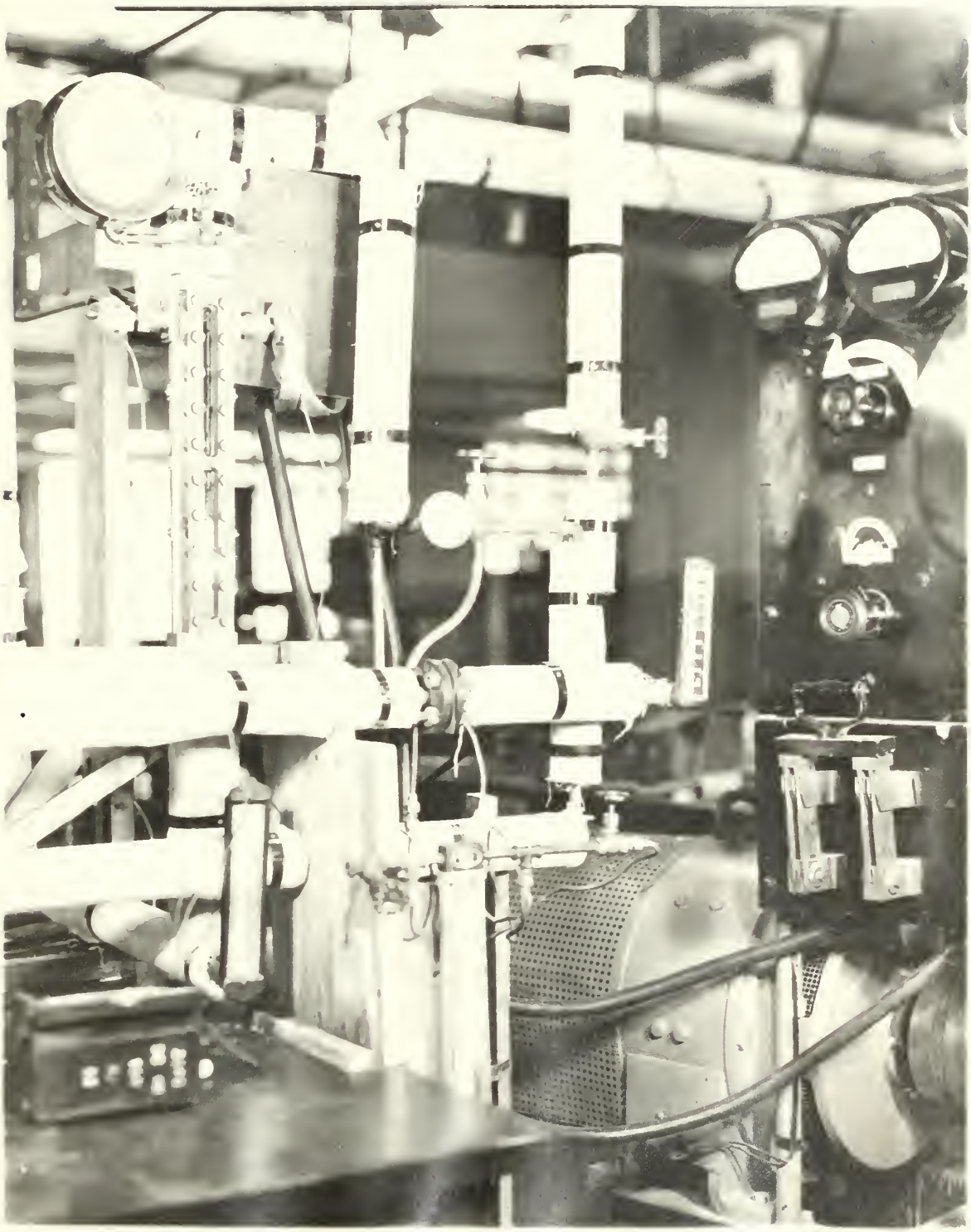

Fig. 2 - Photograph of Apparatus

measurements. The manometer used was a Merriam 20 inch U-manometer, type B-1103. The flow rate was controlled by a valve on the discharge side of the pump.

The test section consisted essentially of a rectangular flow channel, 1/4 inch x 1/2 inch cross section, with electrically heated stainless steel (18-8) strips forming two of the opposite walls. The other two walls were glass which permitted viewing the nucleate boiling bubble formation on the heated strips. The heated strips were 15.0 inches in length, giving an L/y of approximately 60. The inlet approach section was also rectangular, 1/4 inch x 3/8 inch cross section and an L/y of 50. The inlet and outlet sections (Fig. 3) were necessarily narrower, i.e. 3/8 inch instead of 1/2 inch to provide end support for the glasses. Tapered transitions were made at these points. The test section outlet had the same cross sectional dimensions as the inlet but was much shorter, about 3 1/2 inches.

The main part of the test section was mild steel (Fig. 4). This provided a frame to receive the water inlet and outlet sections, the electrical conductors and heating strips, and the glass windows (Jerguson gage glasses, series 5, 17 inch length) which were clamped by modified Jerguson gage glass covers, series 5. Electrical insulation between the stainless steel heating strips and the mild steel frame was achieved by using

measurements. The manometer used was a Merriam 20 inch U-manometer, type 2-1103. The flow rate was controlled by a valve on the discharge side of the pump.

The test section consisted essentially of a rectangular flow channel, 1/8 inch x 1/2 inch cross section, with electrically heated stainless steel (18-8) strips forming two of the opposite walls. The other two walls were glass which permitted viewing the nucleate boiling bubble formation on the heated strips. The heated strips were 15.5 inches in length, giving an L/y of approximately 60. The inlet approach section was also rectangular, 1/4 inch x 3/8 inch cross section and an L/y of 50. The inlet and outlet sections (Fig. 3) were necessarily narrower, i.e. 3/8 inch instead of 1/2 inch to provide and support for the glasses. Tapered transitions were made at these points. The test section outlet had the same cross sectional dimensions as the inlet but was much shorter, about 3 1/2 inches.

The main part of the test section was mild steel (Fig. 4). This provided a frame to receive the water inlet and outlet sections, the electrical connectors and heating strips, and the glass windows (Ferguson gage glasses, series 5, 17 inch length) which were clamped by modified Ferguson gage glass covers, series 5. Electrical insulation between the stainless steel heating strips and the mild steel frame was achieved by [illegible]

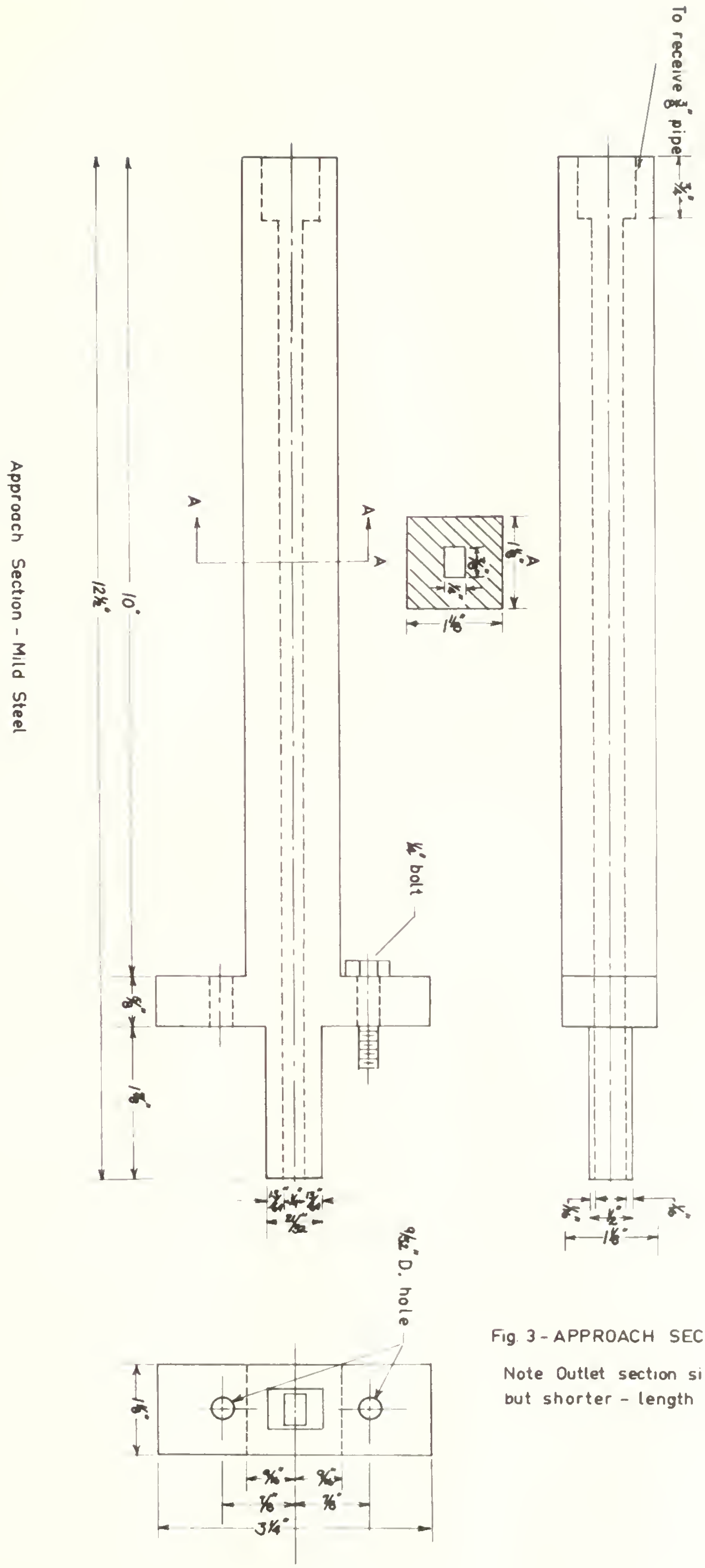

Fig. 3 - APPROACH SECTION

Note Outlet section similar, but shorter - length 3½"

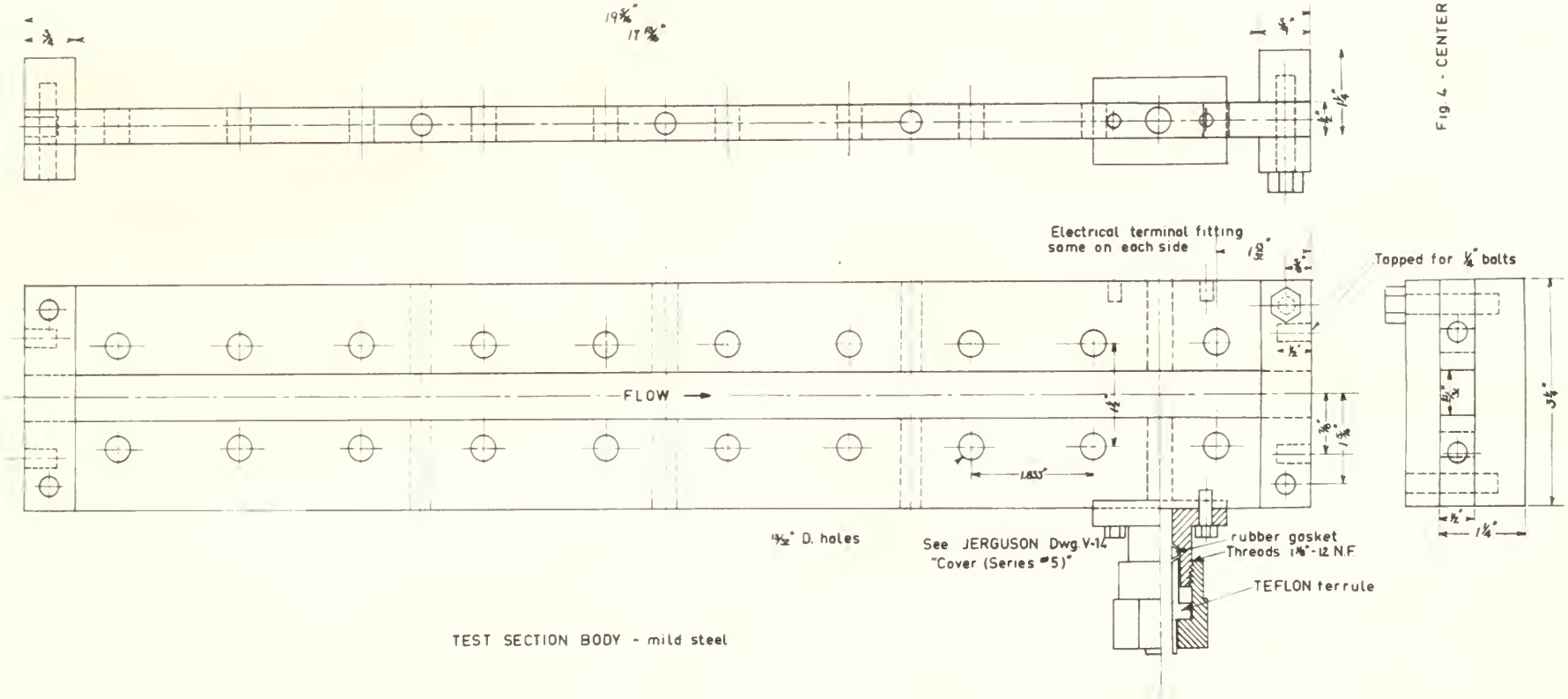

Fig. 4 - CENTER SECTION

Dupont TEFLON plastic. The heater strips were electrically connected in series by a copper bus or connection piece located at the water inlet end of the heater strips (piece "2", Fig. 5). This electrical arrangement was chosen because of the generator characteristics used to provide the electrical power. The power for the heating strips came from a motor-generator set (motor manufacturer, L.J. Land and Co., 220 volts, 60 cycle, 3 phase, 65 amps, 1150 rpm; generator manufacturer, General Electric Corp., model 53A532, 15 volts, 1000 amps).

The distilled water was degassified by boiling in a stainless steel drum heated by a submerged steam coil using 30 pounds saturated steam. Water was transferred to and from this drum, which also served as a system reservoir, by the Westinghouse pump.

Difficulty was experienced with very small rust particles, apparently from the steel jacketed preheaters, during early runs. A Fulflo Filter BR 10 3/4 Commercial Filter, Corporation, Melrose, Mass., was installed at the 30A pump discharge. This cleared the water satisfactorily.

Originally the test section was in a horizontal position to facilitate the photography. At low flow rates, one to two feet per second in the test section, nucleate boiling bubbles from the lower plate would rise and coalesce with the upper plate bubbles. It was feared that this might cause premature burnout on the upper plate,

Lucent Teflon plastic. The heater strips were electrically connected in series by a copper bus or connection piece located at the water inlet end of the heater strips (Item 727, Fig. 5). This electrical arrangement was chosen because of the generator characteristics used to provide the electrical power. The power for the heating strips came from a motor-generator set (motor manufacturer, U.S. Lamb and Co., 700 volts, 60 cycle, 3 phase, 65 amps, 1150 rpm; generator manufacturer, General Electric Corp., Model 334532, 12 volts, 1000 amps).

The distilled water was degassified by boiling in a stainless steel drum heated by a submerged steam coil using 30 pounds saturated steam. Water was transferred to and from this drum, which also served as a system reservoir, by the Westinghouse pump.

Difficulty was experienced with very small rust particles, apparently from the steel jacketed preheaters, during early runs. A Pollin Filter Co 10 3/4 Commercial Filter, Corporation, Bolrose, Mass., was installed at the 300 psig discharge. This cleared the water satisfactorily.

Originally the test section was in a horizontal position to facilitate the photography. At low flow rates, one to two feet per second in the test section, nucleate boiling bubbles from the lower plate would rise and coalesce with the upper plate bubbles. It was found that this algae cause premature burnout at the upper plate.

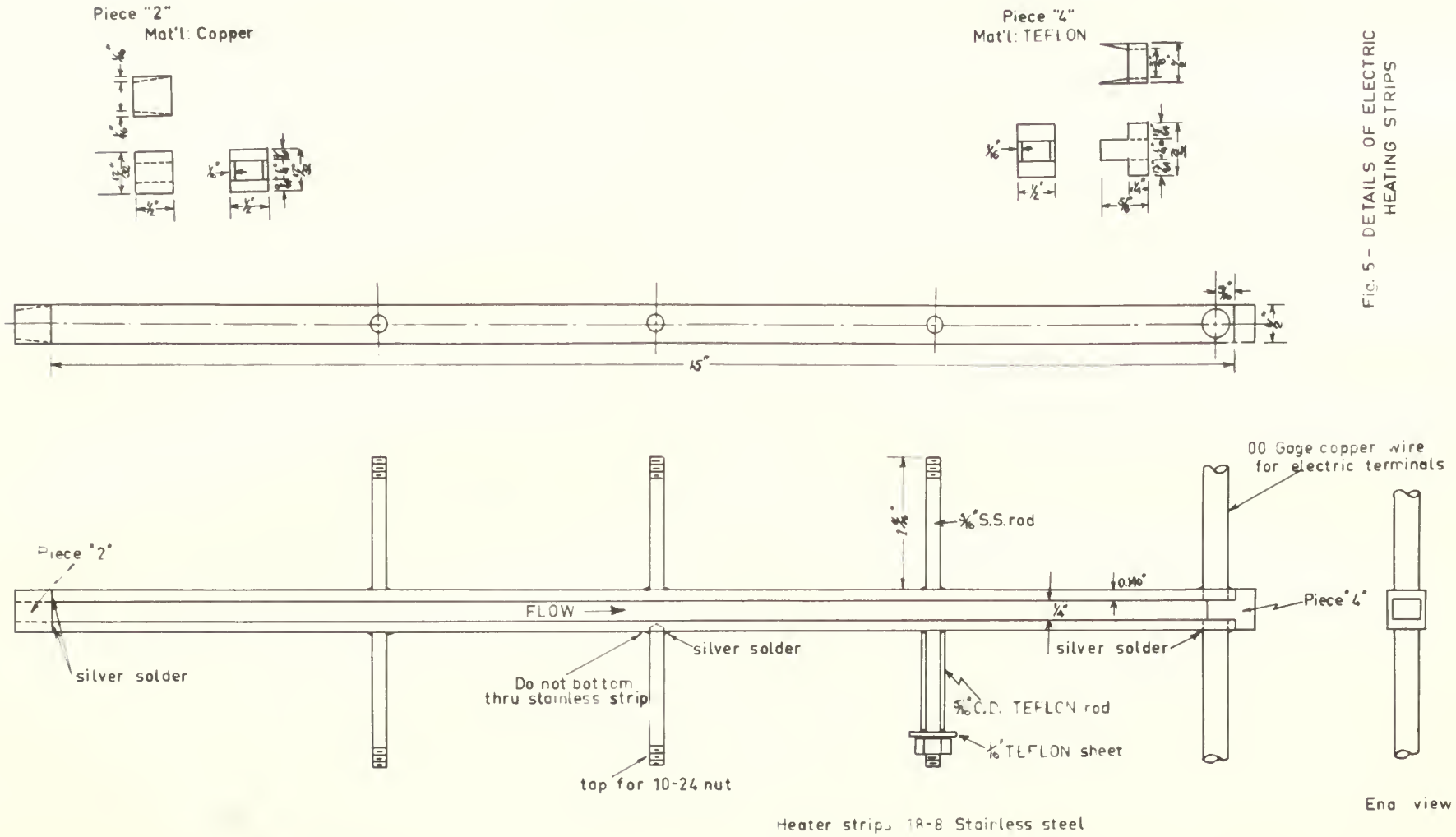

Fig. 5 - DETAILS OF ELECTRIC HEATING STRIPS

so the test section was mounted in a vertical position.

Fig. 5 "Details of Electric Heating Strips" shows the strips as used for the data runs. The first design did not have the six 3/16 inch stainless steel rod supports for the heating strips, but only two small, 5/32 inch, diameter, short, 1/4 inch, stainless steel studs which fastened to a 5/16 inch TEFLON dowel which in turn was tightened by a nut bearing against the outside of the main body of the test section frame. The small studs located at the midpoint of the strips proved inadequate to prevent compressive buckling of the heated strips during preliminary runs. The larger studs improved the situation, but did not eliminate the bowing of the strips completely. The silver solder on the backs of the strips and the thermal capacity of the larger studs undoubtedly caused variations in the electrical current density and the uniformity of the heat generation, but there was no apparent effect on the bubble boundary layer at the stud locations.

Fig 6 Photograph of test section (disassembled)

to the test section was mounted in a vertical position.

Fig. 5 "Measure of Electric Heating Strips" shows the strips as used for the data runs. The first design did not have the six 3/16 inch stainless steel rod supports for the heating strips, but only two small, 3/32 inch, diameter, short, 1/4 inch, stainless steel studs which fastened to a 5/16 inch fairlot dowel which in turn was tightened by a nut bearing against the outside of the main body of the test section frame. The small studs located at the midpoint of the strips proved inadequate to prevent compressive buckling of the heated strips during preliminary runs. The larger studs improved the situation, but did not eliminate the bowing of the strips completely. The silver solder on the bases of the strips and the thermal capacity of the larger studs undoubtedly caused variations in the electrical current density and the uniformity of the heat generation, but there was no apparent effect on the bubble boundary layer at the stud locations.

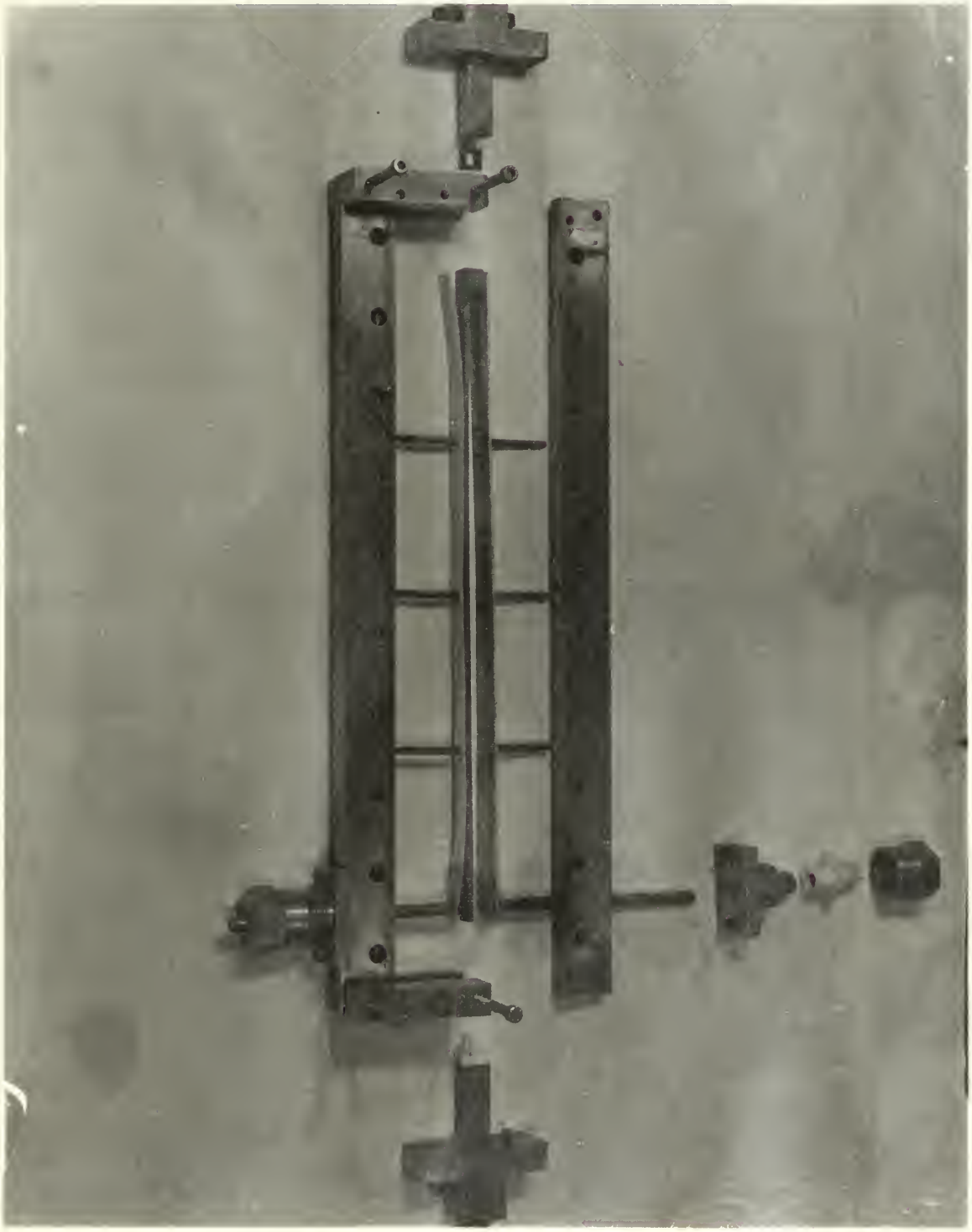

Fig. 6 - Photograph of test section
(disassembled)

EXPERIMENTAL PROCEDURE

The distilled water used in the loop was taken from the degassifier where it had been boiled for one hour before each run. The electrical generator loading and the water flow velocity were set while the electrical preheaters were adjusted to maintain the desired water temperature at the test section inlet.

The voltage was measured across the test section electrical terminals with a Weston D.C. voltmeter, model 45, serial 2849, scale 0-1.5, 15, 150 volts. The ammeter on the motor generator control board gave the current readings. The boiling in the test section would cause appreciable increases in the system pressure. This necessitated readjustments in the flow as the pump characteristics were pressure sensitive. Conditions were allowed to stabilize by observing the test section outlet pressure. This pressure generally steadied within one minute. Photographs were taken with a Graphic View 4 inch x 5 inch still camera having Rapax lens, Wollensak Co., using Panatomic X film. Camera settings used were 1/25 sec and f 22. The test section was backlighted with a microflash light, type 1530-A, General Radio Co., Cambridge, Mass. The light was insufficient to light the entire test section at once, so each photograph covered a length of about eight inches. A typical sequence of photographs

EXPERIMENTAL PROCEDURE

The distilled water used in the loop was taken from the demineralizer where it had been boiled for the hour before each run. The electrical generator loading and the water flow velocity were set while the electrical pressures were adjusted to maintain the desired water temperature at the test section inlet.

The voltage was measured across the test section electrical terminals with a Weston D.C. voltmeter, model 45, serial 2640, scale C-1.5, 15, 150 volts. The ammeter on the motor generator control board gave the current readings. The boiling in the test section would cause appreciable increases in the system pressure. This necessitated readjustments in the flow as the pump characteristics were pressure sensitive. Conditions were allowed to stabilize by observing the test section outlet pressure. This pressure generally standed within one minute. Photographs were taken with a Graphic Flex 4 inch x 5 inch still camera using Kapar lens, Bellsnack Co., using Panatomic X film. Camera settings used were 1/25 sec and f 24. The test section was backlighted with a microframe light, type 1530-A, General Radio Co., Cambridge Mass. The light was insufficient to light the entire test section at once, so each photograph covered a length of about eight inches. A typical isochrone of photographs

is appended as Fig. 7, 8 and 9. All of the photographs and negatives are in the possession of Prof. J.A. Clark. Time was not available for the intended motion picture study.

Fig. 7 - v 1 ft/sec
Q/A 83,000 Btu/hr ft^2

Fig. 8 v 1 ft/sec
Q/A 166,000 Btu/hr ft^2

Fig. 9 - v 1 ft/sec
Q/A 250,000 Btu/hr ft^2

DISCUSSION OF RESULTS

An attempt was made to correlate the physical conditions in the channel such as heat flux density, flow velocity and fluid enthalpy, at the point where the two bubble boundary layers met or intermingled. This was not successful and it is believed that the principal difficulty was in establishing or defining the actual location of the junction. Before the vapor bubbles grow to a size which is about half of the channel width, the bubble is influencing the boundary layer on the opposite strip. With bubbles of this size, the photographs show that the flow is not symmetrical. A bubble deflects the water toward the opposite strip and seems to wipe off the bubbles or reduce the boundary layer thickness there.

The quantity h_x is the calculated bulk enthalpy at the point of intersection of the bubble boundary layers and is equal to the inlet enthalpy h_i plus the energy added per pound by the heater strips between the inlet and the point

$$h_x = h_i + 2\left(\frac{Q}{A}\right)\frac{A_x}{w}$$

where A_x is the area of one strip between inlet and the point x, and w is mass flow rate through the channel. The experimental conditions for the various runs is tabulated on pages 25, 26, and 27. The following data was calculated for the runs indicated:

Discussion of results

In attempt was made to determine the position where diffusion in the mixture was at least than unity. For variable and fixed velocity, at the point where the two media boundary layers were at coincidence. This was an considerable one is to achieve this the optimum difficulty was in attempting to satisfy the wedge length of the jacket. Since the major resistance was of a film which is upon fall of the desired slope, the ability to determine the boundary layer on the opposite wall. The thickness of data also, the thermocouple show that the flow is not symmetrical. A better suitable the flow boundary for opposite wall and hence to rule off the operation of where the boundary layer thickness there.

The quantity δ_g in the calculation was actually at the point of intersection of the mixing boundary layers and is equal to the point average δ_g plus the average value per point to the inner mixing between the film and the point.

$$\delta_g = \delta_1 + 2\left(\frac{\delta}{A}\right)\frac{A_x}{\omega}$$

where δ_1 is the area of the point boundary layer at the point 1, and δ is the area that lower the boundary. The mathematical conditions for the mixing zone is identical on point δ_1, δ_2, and δ_3. The following data was obtained for the two layers laminated.

Picture		Picture	
7	-.062	14	-.031
8	-.064	15	-.034
9	-.027	16	-.035
10	-.030	17	-.040
11	-.053	18	-.056
12	-.043	19	-.039
13	-.031	20	-.048

The quantities h_f, the saturated liquid enthalpy, and h_{fg}, latent heat of evaporation correspond to the pressure measured at the test section outlet. No hydrostatic correction was made. It is significant that all of the points selected showed a negative "quality" or a bulk enthalpy less than the saturated enthalpy at the point where the vapor appears to be blocking the channel.

It must be remembered, however, that the bubbles are actually three dimensional rather than two as is implied here when the point of intersection is assumed. The actual "quality" is undoubtedly less than the value calculated since all the energy generated in the strips was assumed to be transferred to the fluid. There were certainly heat losses through the back of the heating strips both by conduction and by boiling of water which leaked on to the back of the strip. No theoretical calculations were made to estimate the magnitude of this loss nor was a heat balance attempted

Picture		Picture	
7	-.002	14	-.034
8	-.004	15	-.034
9	-.027	16	-.035
10	-.030	17	-.040
11	-.033	18	-.036
12	-.043	19	-.039
13	-.031	20	-.048

The quantities h_i, the separation liquid quantity, and h_{ik}, intent heat of evaporation corresponds to the pressure measured at the test section outlet. No hydrostatic correction was made. It is significant that all of the points calculated amount a negative "quality" or a weak enthalpy less than the saturated enthalpy at the point where the vapor appears to be blocking the channel.

It must be remembered, however, that the quantities are actually three dimensional points that lie off to implied here when the point of intersection is assumed. The actual "quality" is undoubtedly less than the value calculated since all the energy generated in the strips was assumed to be transferred to the fluid. There were certainly heat losses through the base of the heating strips both by conducting and by boiling of water which leaves up to the base of the strip. No separation calculations were made to estimate the magnitude of this loss nor was a heat balance attempted

on the section because of inadequate instrumentation. It is believed that the losses are less than ten percent.

Several "exploratory" runs were made in an effort to achieve a higher quality at the test section outlet. No photographs were taken. With $Q/A = 455,000$ Btu/hr ft^2, $v = 1$ ft/sec, $t_i = 170^\circ$ and $p = 45$ psia, the calculated quality at outlet was about - 1.4%. The last few inches of the channel appeared to be almost all vapor. $Q/A = 450,000$ Btu/hr ft^2, $v = 0.8$ ft/sec, $t_i = 184$ and $p = 53$ psia gave a pulsating flow with slugs of vapor surging up the channel. The calculated outlet quality was - 4.7%. The highest quality achieved was - 14.4% with $Q/A = 440,000$ Btu/hr ft^2, $v = 0.5$ ft/sec, $t_i = 196^\circ$, and $p = 60$ psia. With these conditions the upper two thirds of the test section was mostly vapor with violent boiling in the bottom third.

Plots were made of δ, the thickness or height of the bubble boundary layer, against a parameter H, which expressed the subcooling of the bulk liquid at the location where was measured. H is the same negative "quality" or subcooling spoken of previously.

$$H \equiv \frac{h_\delta - h_f}{h_{fg}}$$

where

$$h_\delta = h_i + 2\left(\frac{Q}{A}\right)\frac{A_\delta}{\omega}$$

and h_δ is the calculated enthalpy at the point where δ was measured. The value of H was also calculated ignoring all heat losses. As H is a calculated quantity, the experimental uncertainty is of interest. With the following experimental variations:

flow velocity	$\pm$ 0.1 ft/sec for v = 1 ft/sec
pressure	$\pm$ 0.5 psia
inlet temperature	$\pm$ 0.5°F
generator current	$\pm$ 5.0 amps

the resulting uncertainty in H can be estimated. Taking run #29, which is Fig. 8, as an example where δ = .083 inches at a distance x = 9.35 inches from the beginning of the heated strip.

$Q = 8.3 \text{ volts} \times 600 \pm 5 \text{ amps} = 4.72 \pm 0.4 \text{ Btu/sec}$

$w = .11 \pm .01 \text{ lb/sec}$

$h_\delta = h_i + Q \cdot \frac{1}{w}\left(\frac{x}{L}\right)$ L = 14.7" length of heated strip

with $t_i = 200°F \pm 0.5°F$, $h_i = 168.0 \pm 0.5$ Btu/lb

since p = 41 $\pm$ 0.5 psia

$h_f = 237.5 \pm 0.7$ Btu/lb

$h_{fg} = 932.6 \pm 0.5$ Btu/lb

$$H = \frac{h_\delta - h_f}{h_{fg}}$$

and h_δ is the calculated enthalpy at the point where δ was measured. The value of H was also calculated ignoring all heat losses. As H is a calculated quantity, its experimental uncertainty is of interest. With the following experimental variations:

flow velocity	± 0.1 ft/sec for v = 1 ft/sec
pressure	± 0.5 psia
inlet temperature	± 0.5°F
generator current	± 5.0 amps

the resulting uncertainty in H can be estimated. Taking run #37, which is Fig. 8, as an example where δ = .083 inches at a distance x = 9.25 inches from the beginning of the heated strip.

$h_\delta = h_1 + Q \cdot \frac{1}{\omega}\left(\frac{x}{L}\right)$ L = 14.7" length of heated strip

with t_1 = 200°F ± 0.5°F, h_1 = 168.0 ± 0.5 Btu/lb

since p = 21 ± 0.5 psia

h_{fg} = 837.3 ± 0.7 Btu/lb

h_{fg} = 832.8 ± 0.7 Btu/lb

$$C = \frac{h_\delta - h_f}{h_{fg}}$$

$$H = \frac{(195.3 \pm 3.3) - (237.5 \pm 0.7)}{932.6 \pm 0.5}$$

$$H = 0.045 \pm .003$$

This shows an uncertainty of about 6% in H. The largest variations were in the water velocity and the generator current measurements, consequently the scatter was appreciably greater for the low flow and low power runs. This is quite possibly the explanation for the seeming inconsistencies shown on Fig. 10 where Q/A = 83,000 Btu/hr ft^2 and the 3 ft/sec is to the right of the 2 ft/sec run.

The plots of δ vs h show that the growth of the bubble boundary layer is as would be expected. It is less for the greater subcooling and higher velocities while greater for the higher heat flux densities. These variations are given quantitatively by the graphs. Since the general shape of the various curves is similar, it was thought that a correlation for the nucleation points (i.e. $\delta = 0$) might be found. As the pressure was different for the various runs, a pressure parameter for nucleation was sought. Using the liquid superheat at incipient nucleation, a term was added to the "subcooling" parameter H used previously. If

$$(t_w^* - t_f) = f(p)$$

where t_w^* is the wall temperature at the point of nucleation and t_f is the bulk fluid temperature.

$$h_w^* - h_f^* = f(p)$$

$$H = \frac{(142.3 \pm 3.3) - (237.5 \pm 0.7)}{732.6 \pm 0.5}$$

$$H = 0.045 \pm .003$$

If p is assumed constant then h_f and h_{fg} are constant,

$$\frac{(h_w - h_f)^* + (h_f - h_\delta)}{h_{fg}} = \frac{h_w^* - h_\delta^*}{h_{fg}}$$

$$M \equiv \left(\frac{h_w - h_f}{h_{fg}}\right) - H \quad \text{where} \quad H = \frac{h_\delta^* - h_f}{h_{fg}}$$

Values for $t_w^* - t_f$ as a function of pressure were taken from Figure IV-C-2 "Maximum Experimental and Theoretical Degree of Liquid Superheat" from ref. (3).

The experimental superheat curve for the stainless steel - water system was used. The pressure nucleation correction was applied to smoothed curves of δ vs M. The resulting correlation is shown in Fig. 21. While it is true that this resulted in a closer grouping of the data, such a high value of superheat ($\sim 150^\circ F$) obtained in an experiment where the water was very clean, unheated and static is unlikely in a moving fluid being heated. It is felt that a superheat of about thirty degrees would be more reasonable. Any such lower value of superheat would tend to scatter the curves more. It is apparent that a generalized correlation is yet to be gained.

If δ is assumed constant then h_f and h_{fg} are constants,

$$\frac{h_w^* - h_\delta^*}{h_{fg}} = \frac{(h_w - h_f)^* + (h_f - h_\delta)}{h_{fg}}$$

$$\frac{h_\delta^* - h_f}{h_{fg}} = H \quad \text{where} \quad H - \left(\frac{h_w - h_f}{h_{fg}}\right) \equiv M$$

Values for $t_w^* - t_f$ as a function of pressure were taken from Figure IV-6-2 "Maximum Experimental and Theoretical Curves of Liquid Superheat" from ref. (3).

The experimental superheat curve for the stainless steel - water system was used. The pressure compensation correlation was applied to obtained curves of δ vs θ. The resulting correlation is shown in Fig. 21. While it is true that this resulting in a closer grouping of the data, such a high value of superheat ($\sim 150°F$) obtained in an experiment where the water was very clean, deaerated and easily is unlikely in a cooling fluid being heated. It is felt that a superheat of about thirty degrees would be more reasonable, nor such lower value of superheat would tend to bounce the curves more. It is apparent that a generalized correlation is yet to be gained.

LIST OF SYMBOLS

A_δ	area of heater strip from inlet to point where δ was measured	(sq.in.)
A_x	area of heater strip from inlet to point where $\delta = 1/2\ y$	(sq.in.)
	height of bubble boundary layer	(in)
h_δ	fluid enthalpy at point where δ is measured	(Btu/lb)
h_f	enthalpy of liquid	(Btu/lb)
h_{fg}	latent heat of evaporation	(Btu/lb)
h_i	fluid enthalpy at test section inlet	(Btu/lb)
h_x	fluid enthalpy at point x	(Btu/lb)
H	"subcooling" parameter $\equiv \frac{h_\delta - h_f}{h_{fg}}$	
L	length of heated strip 14.7"	
M	"nucleation - subcooling" parameter $\equiv \frac{(h_w - h_f^*) - (h_\delta^* - h_f)}{h_{fg}}$	
p	test section outlet pressure	(psia)
Q/A	heat flux density	(Btu/hr ft^2)
t_w	temperature of heated wall	($^\circ$F)
t_f	temperature of fluid	($^\circ$F)
v	flow velocity	(ft/sec)
w	mass flow rate	(lb/sec)
x	distance from inlet where δ is measured	(in)
y	spacing between heater strips	(in)
*	indicates conditions at bubble nucleation	

LIST OF SYMBOLS

δ^* Area of heater strip from point of origin where δ vanishes (sq.in.)

δ^* area of heater strip from inlet to point where $\delta = 1/2\,\gamma$ (sq.in.)

δ Relative of thermal boundary layer (in)

δ Fluid velocity at point where δ is measured (ft/sec)

μ Viscosity of fluid (lbm/ft)

μ_f Latent heat of evaporation (Btu/lb)

ρ Fluid density at heat transfer point (lbm/ft³)

ρ_f Fluid density at point x (lbm/ft³)

Π "Pressure" parameter $\equiv \dfrac{\rho_f - \rho_f^*}{\rho_f^*}$

Π Length of heated strip (in)

Π Transformation - hydrodynamic parameter $\equiv \dfrac{(\rho_w - \rho_f^*) - (\rho_f^* - \rho_f)}{\rho_f^*}$

ρ Heat transfer rotary parameter (Btu)

ρ_s Heat flux density (Btu/hr ft²)

ρ_f Temperature of heated wall (°F)

ρ_f Temperature of fluid (°F)

ρ Flow velocity (ft/sec)

ρ Mean flow rate (in/sec)

x distance from inlet where δ is measured (in)

y spacing between heater strips (in)

γ indicates conditions in boiling nucleation

Experimental and Calculated Data on the Bubble Boundary Layer

Fict.	Volts	Amps	Q/A	v ft/sec	t_i °F	p psia	δ in.	x in.	-H
#1	4.5	330	49,000	1	180	15	.00	5.11	.029
							.04	7.85	.026
							.081	9.27	.025
							.081	10.96	.022
#2	5.9	430	83,000	1	180	17	.00	4.26	.035
							.016	5.78	.032
							.032	8.30	.028
							.089	9.11	.027
							.113	10.71	.025
#3	7.8	565	147,000	1	180	28	.00	2.75	.067
							.04	3.59	.064
							.056	6.49	.056
							.072	8.15	.052
							.113	10.23	.046
#5	8.4	605	166,000	2	180	22	.00	2.75	.050
							.024	4.27	.047
							.032	5.89	.044
							.064	8.05	.041
							.072	10.01	.038
#6	10.3	730	250,000	2	180	26	.00	2.25	.061
							.034	3.01	.059
							.034	4.84	.055
							.052	7.0	.050
							.06	9.15	.045
							.086	10.89	.041
#7	13.5	920	416,000	2	180	48	.00	1.75	.100
							.075	8.16	.075
							.09	9.05	.070
							.11	10.41	.066
#8	15.0	1,000	500,000	2	180	56	.00	1.75	.111
							.082	7.75	.082
							.108	8.75	.078
							.125	9.06	.076

Fict.	Volts	Amps	Q/A	v ft/sec	t_i °F	p psia	δ in.	x in.	-H
#9	8.3	605	166,000	3	180	17	.00	2.87	.038
							.092	8.26	.033
							.10	9.53	.031
							.125	10.87	.030
							.083	11.75	.029
							.117	12.71	.028
#10	10.3	730	250,000	3	180	20	.00	2.75	.046
							.043	8.27	.038
							.078	9.47	.036
							.086	9.71	.036
							.104	10.85	.034
							.12	12.55	.031
#11	12.3	850	333,000	2	180	36	.00	1.87	.083
							.117	8.45	.070
							.109	9.71	.067
							.107	10.62	.065
							.117	11.57	.063
#12	12.3	850	333,000	3	180	26	.00	2.25	.061
							.066	7.66	.050
							.083	8.34	.049
							.108	9.59	.046
							.117	10.33	.045
#13	12.3	850	333,000	4	180	20	.00	2.75	.046
							.042	7.85	.038
							.066	9.0	.036
							.083	9.66	.036
							.10	10.96	.034
#14	12.3	850	333,000	5	174	17	.00	3.0	.040
							.041	7.75	.040
							.066	8.84	.039
							.066	9.75	.038
#15	12.2	855	333,000	5	180	19	.00	2.87	.047
							.069	8.94	.037
							.078	9.99	.035
							.112	11.51	.034
							.129	13.42	.031

Experimental and Calculated Data on the Bubble Boundary Layer

Pict.	Volts	Amps	q/A	v ft/sec	t_i °F	p psia	δ in.	x in.	-h
#16	13.5	930	416,000	5	180	22	.00	3.0	.049
							.067	8.0	.042
							.058	8.5	.041
							.075	8.84	.040
							.075	9.82	.039
							.075	10.02	.038
							.067	11.8	.036
							.084	12.0	.034
#17	13.4	925	416,000	4	180	24	.00	2.37	.058
							.042	8.29	.046
							.10	8.53	.046
							.117	9.03	.045
							.083	9.46	.044
							.092	9.87	.043
							.133	10.29	.042
							.10	11.21	.040
							.133	11.82	.039
#18	13.5	925	416,000	3	180	32	.00	1.87	.076
							.084	7.99	.058
							.108	8.71	.056
							.125	9.28	.055
#20	14.5	990	476,000	4	180	29	.00	2.0	.068
							.058	8.09	.055
							.067	8.75	.054
							.117	9.3	.052
							.092	10.0	.051
							.092	11.3	.048
							.108	12.0	.046
#22	5.9	430	83,000	1	200	25	.00	2.75	.038
							.067	8.01	.030
							.075	9.05	.028
							.091	9.75	.027
							.108	11.0	.025
							.101	12.09	.023
							.091	14.0	.021
#24	5.9	430	83,000	2	200	20	.00	2.12	.027
							.042	7.67	.023
							.067	8.12	.023
							.10	8.67	.023
							.067	8.87	.023
							.067	9.37	.022
							.05	9.62	.022
							.075	9.76	.022
							.083	10.28	.021
							.083	10.43	.021
							.075	12.82	.019
							.092	14.22	.018
							.10	14.82	.018

Pict.	Volts	Amps	q/A	v ft/sec	t_i °F	p psia	δ in.	x in.	-h
#25	5.8	435	83,000	3	200	20	.00	4.37	.026
							.042	6.45	.027
							.066	6.87	.026
							.033	7.56	.025
							.067	8.04	.025
							.067	8.71	.025
							.083	9.0	.025
							.075	9.75	.024
							.117	10.42	.024
							.108	11.67	.023
							.108	12.84	.023
#26	8.3	600	166,000	4	200	21	.00	4.12	.032
							.05	8.93	.027
							.033	9.26	.027
							.067	9.96	.027
							.108	10.67	.026
							.10	11.12	.026
							.075	12.64	.025
							.108	13.62	.024
							.10	14.12	.024
#27	8.3	600	166,000	3	200	23	.00	2.75	.037
							.066	7.84	.032
							.075	8.33	.031
							.058	9.03	.030
							.067	9.35	.030
							.083	9.92	.029
							.075	10.91	.028
							.15	11.68	.028
							.10	12.95	.026
#28	8.3	600	166,000	2	200	27	.00	2.37	.049
							.067	7.95	.040
							.075	8.21	.040
							.117	8.41	.040
							.083	9.17	.038
							.108	9.87	.037
#29	8.3	600	166,000	1	200	41	.00	2.0	.068
							.054	7.76	.050
							.075	8.17	.049
							.058	8.53	.048
							.10	8.75	.047
							.083	9.35	.045
							.10	9.75	.044
							.125	10.35	.042
							.12	11.96	.037
#30	10.5	725	250,000	1	200	56	.00	1.5	.096
							.067	7.93	.060
							.084	8.25	.058
							.10	9.21	.054
							.108	9.75	.052
							.117	10.35	.048

Calculated Values of the "Nucleation and Subcooling" Parameter M for smoothed curves of δ

Fict.	δ	$(t_w-t_f)^*$	M	Fict.	δ	$(t_w-t_f)^*$	M
#2	0	160	.200	#16	0	150	.206
	.05		.193		.05		.197
	.10		.191		.10		.194
#3	0	142	.215	#17	0	147	.212
	.05		.206		.05		.201
	.10		.198		.10		.197
#6	0	144	.197	#18	0	136	.220
	.05		.188		.05		.206
	.10		.184		.10		.200
#7	0	120	.229	#20	0	140	.216
	.05		.204		.05		.202
	.10		.198		.10		.198
#8	0	114	.235	#22	0	145	.190
	.05		.212		.05		.183
	.10		.203		.10		.178
#9	0	160	.203	#24	0	154	.187
	.05		.198		.05		.184
	.10		.193		.10		.182
#10	0	154	.222	#25	0	154	.187
	.05		.208		.05		.184
	.10		.203		.10		.184
#11	0	131	.223	#26	0	152	.189
	.05		.211		.05		.185
	.10		.208		.10		.183
#12	0	144	.212	#27	0	148	.192
	.05		.203		.05		.1855
	.10		.198		.10		.183
#13	0	154	.206	#28	0	142	.199
	.05		.198		.05		.191
	.10		.194		.10		.1855
#15	0	156	.216	#29	0	126	.203
	.05		.208		.05		.184
	.10		.204		.10		.179
				#30	0	114	.214
					.05		.185
					.10		.178

GRAPHIC PLOTS OF DATA

The following figures are arranged first for constant heat flux density Q/A with varying flow velocities to show the velocity effect on the growth of the bubble boundary layer for different subcoolings. The data was next cross-plotted at a constant flow velocity to show the effect of changing heat flux density against subcooling.

Fig. 10 - Q/A = 83,000 Btu/hr ft^2

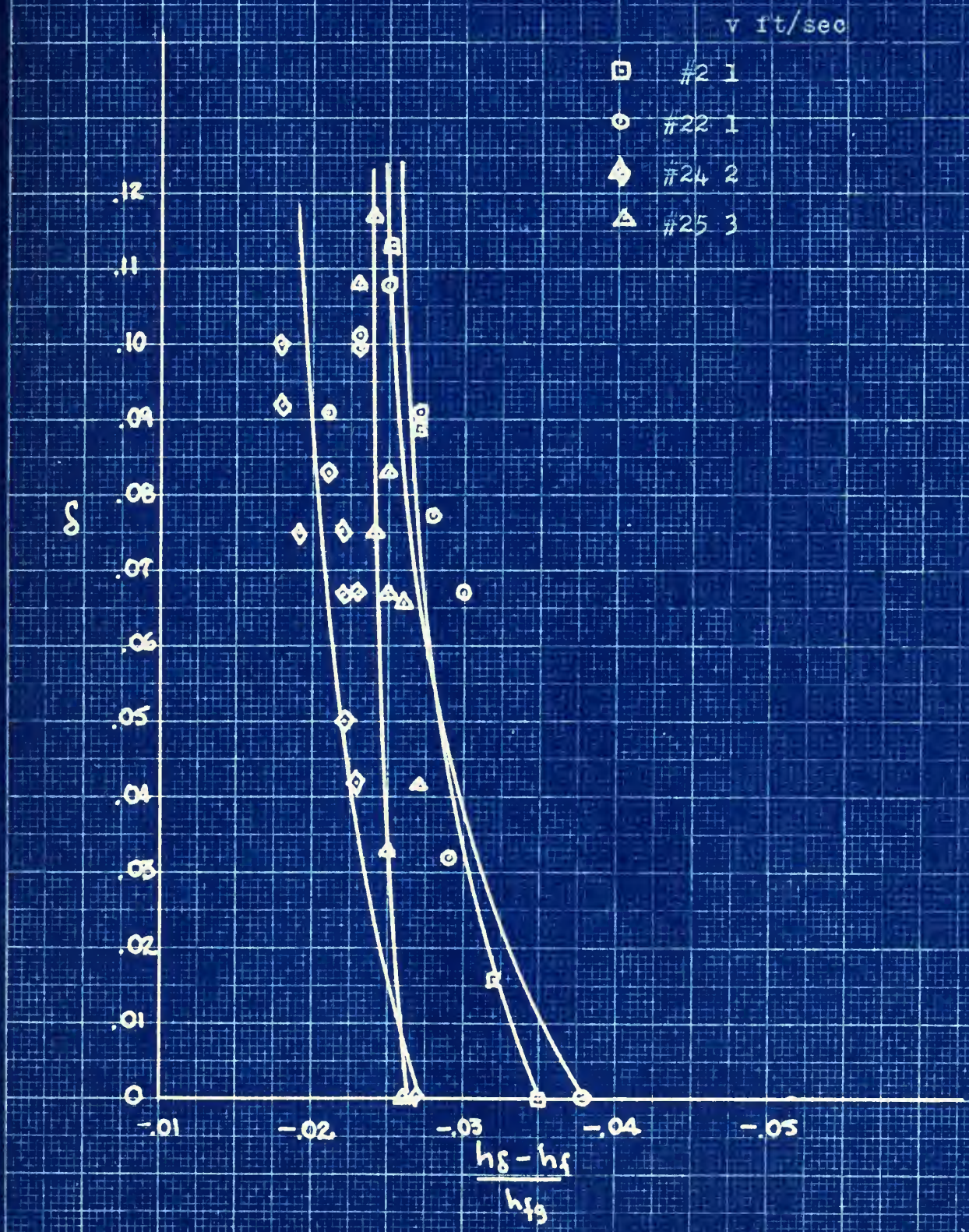

Fig. 11 - Q/A = 166,000 Btu/hr ft^2

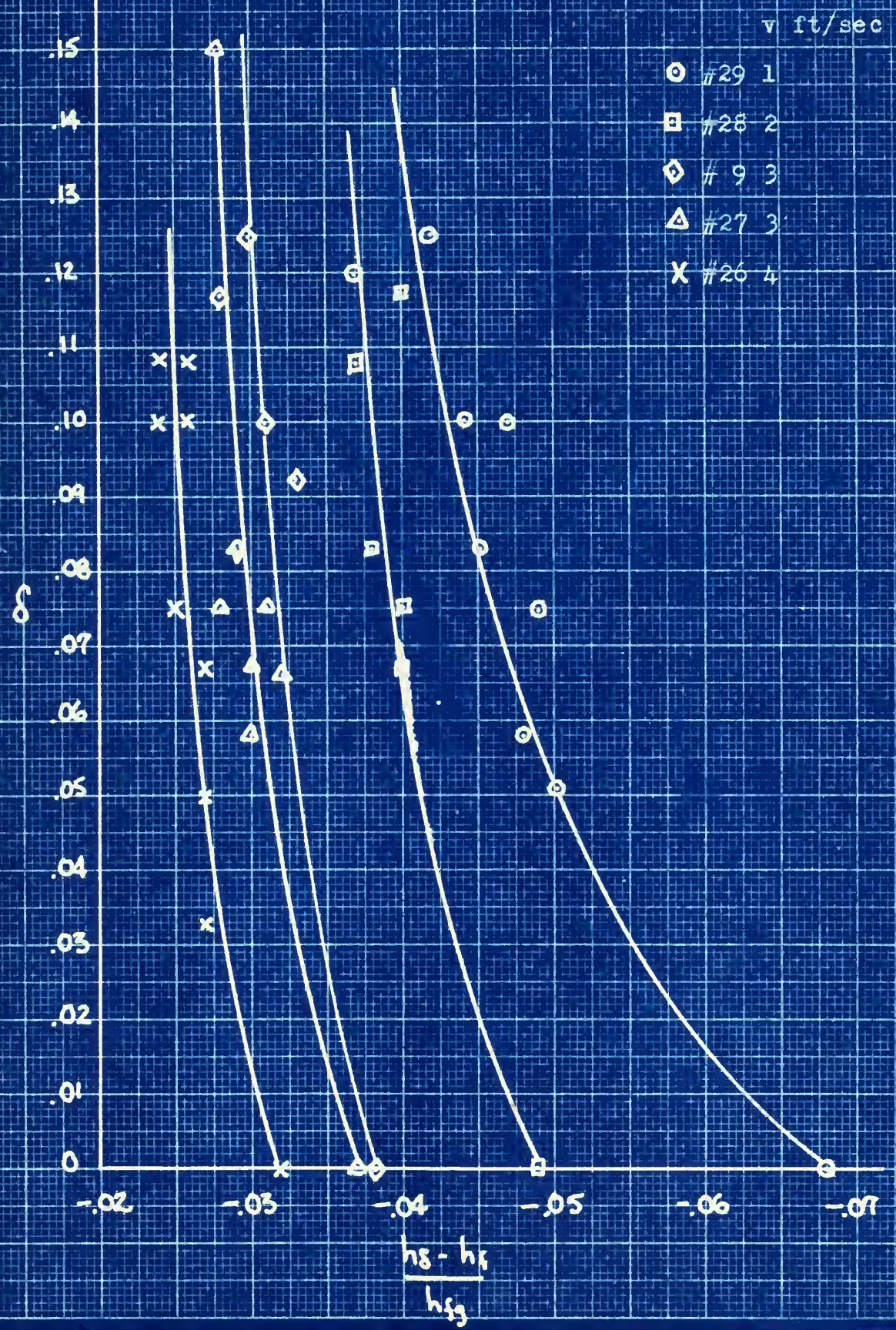

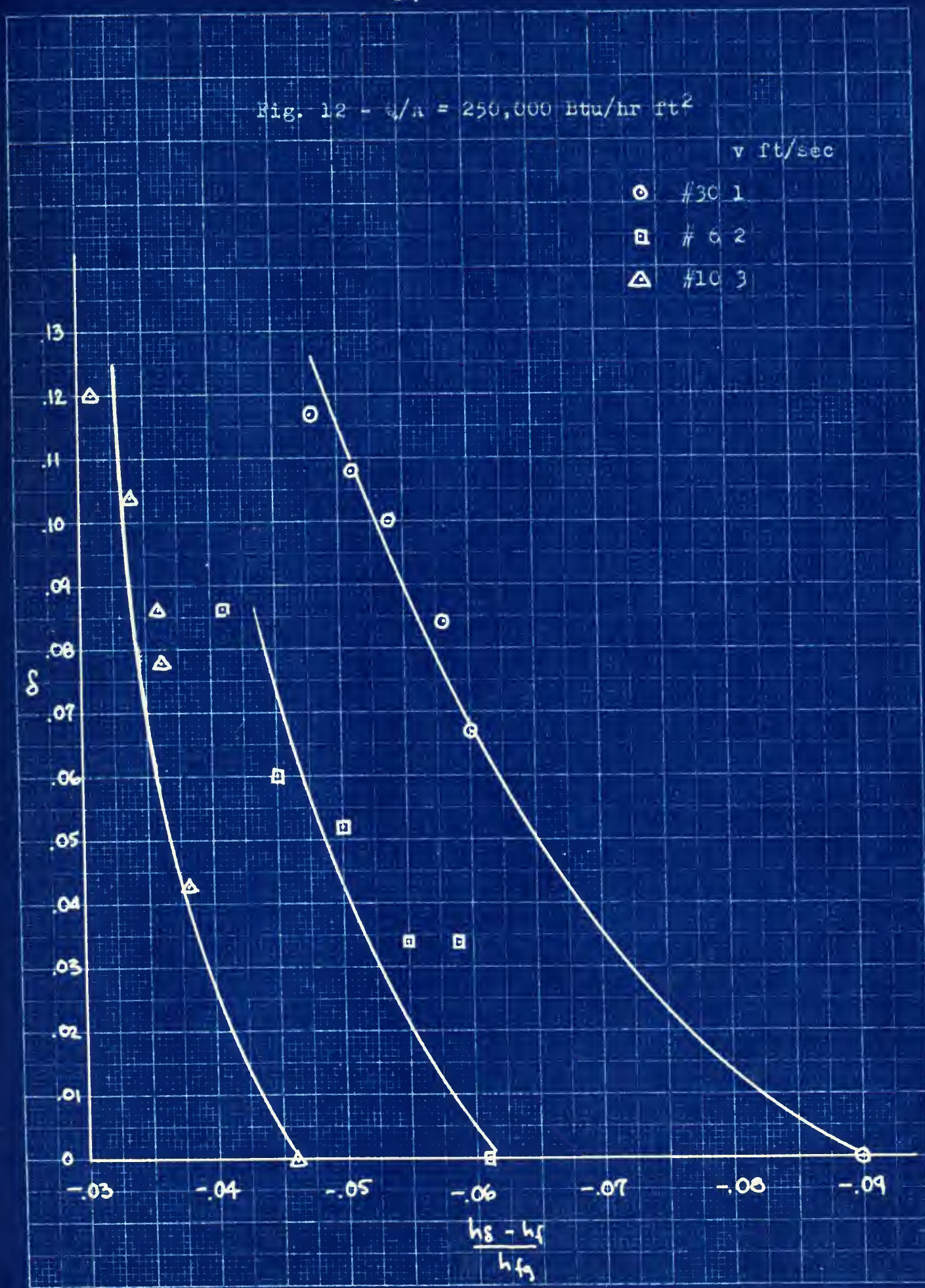
Fig. 12 - q/A = 250,000 Btu/hr ft²
v ft/sec
#30 1
6 2
#10 3
δ
.13
.12
.11
.10
.09
.08
.07
.06
.05
.04
.03
.02
.01
0
-.03
-.04
-.05
-.06
-.07
-.08
-.09
hs - hf
hfg

Fig. 13 - Q/A = 333,000 Btu/hr ft^2

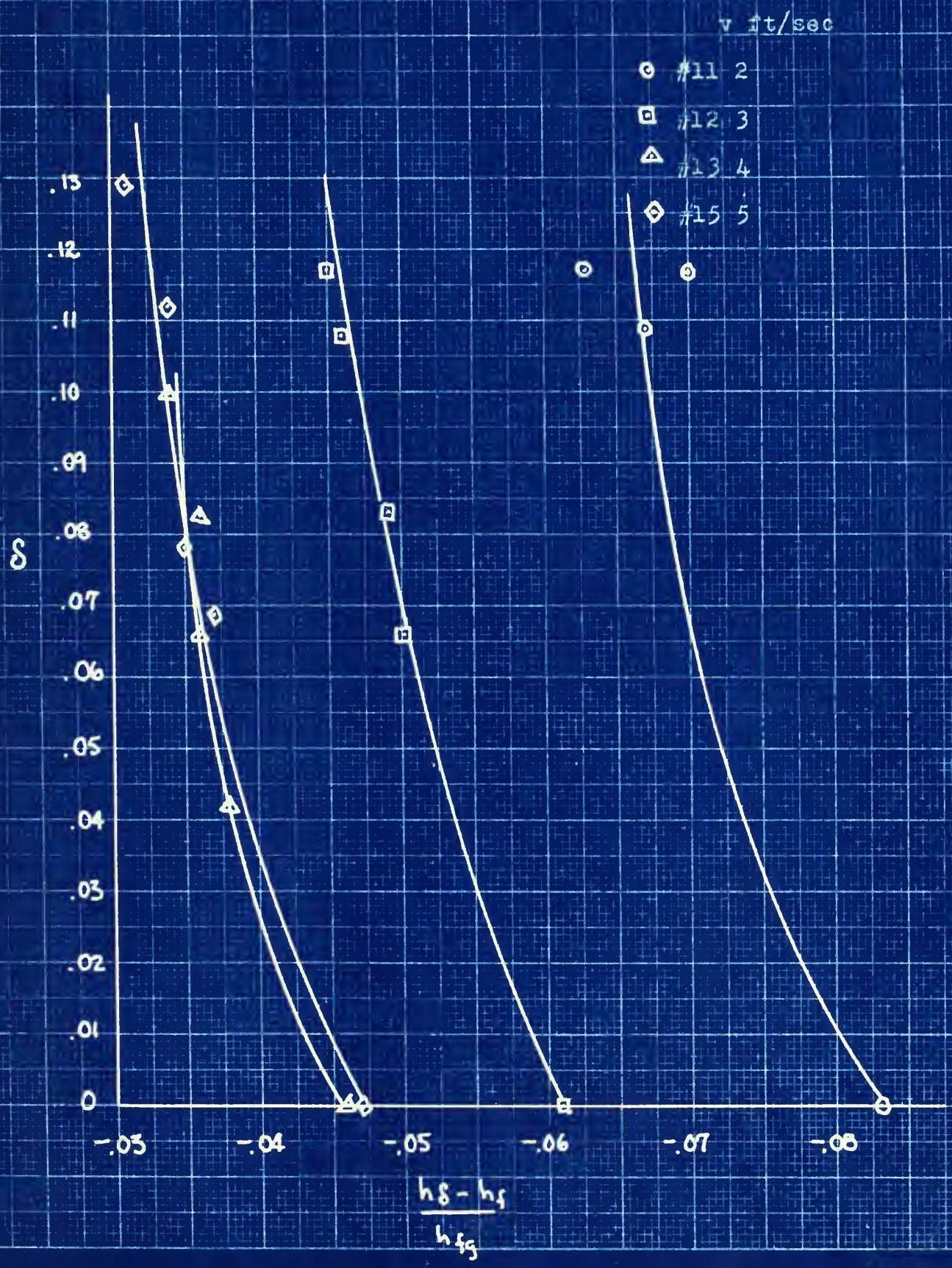

Fig. 14 - Q/A = 416,000 Btu/hr ft^2

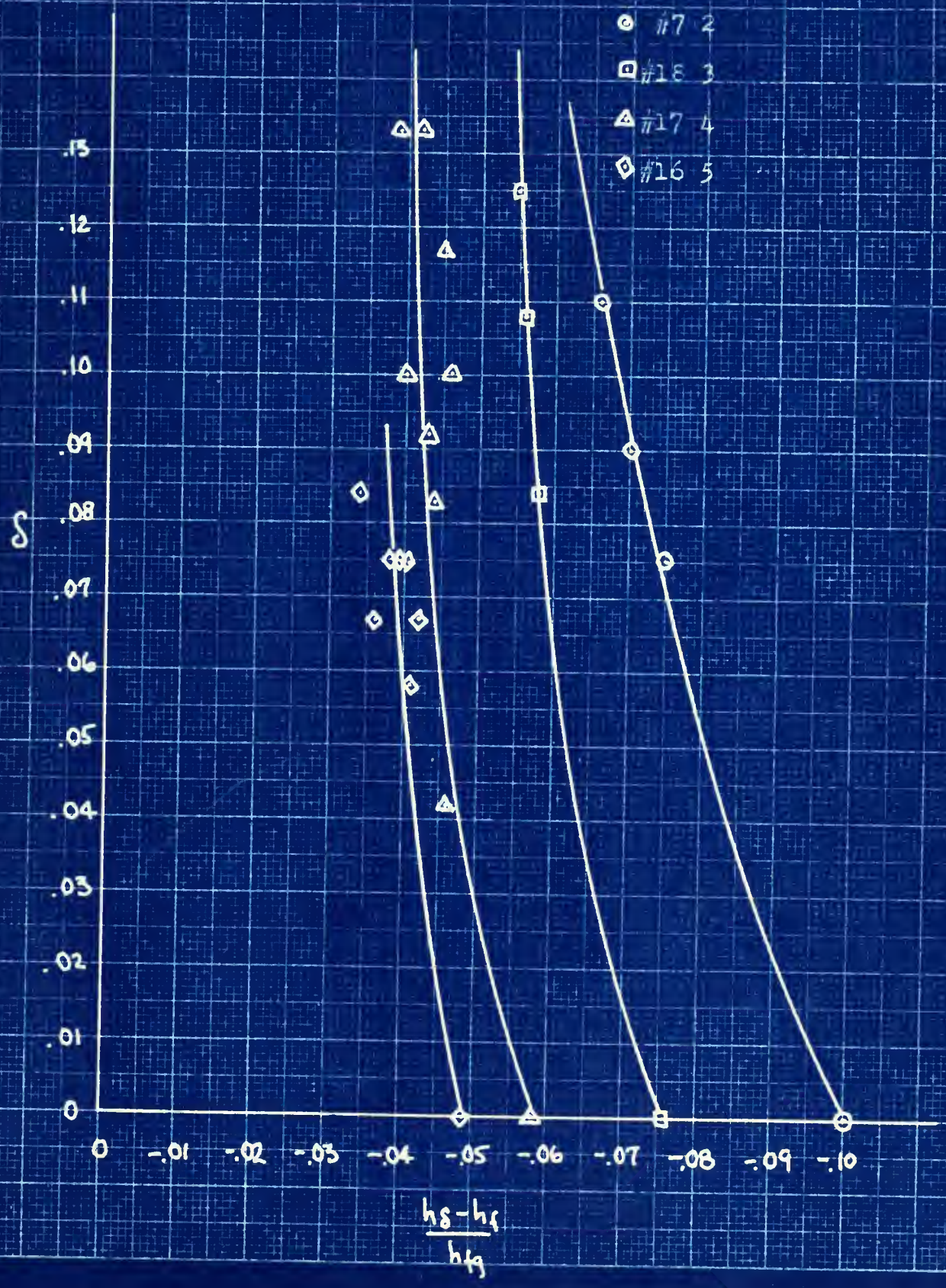

Fig. 15 - Q/A = 475,000 Btu/hr ft^2

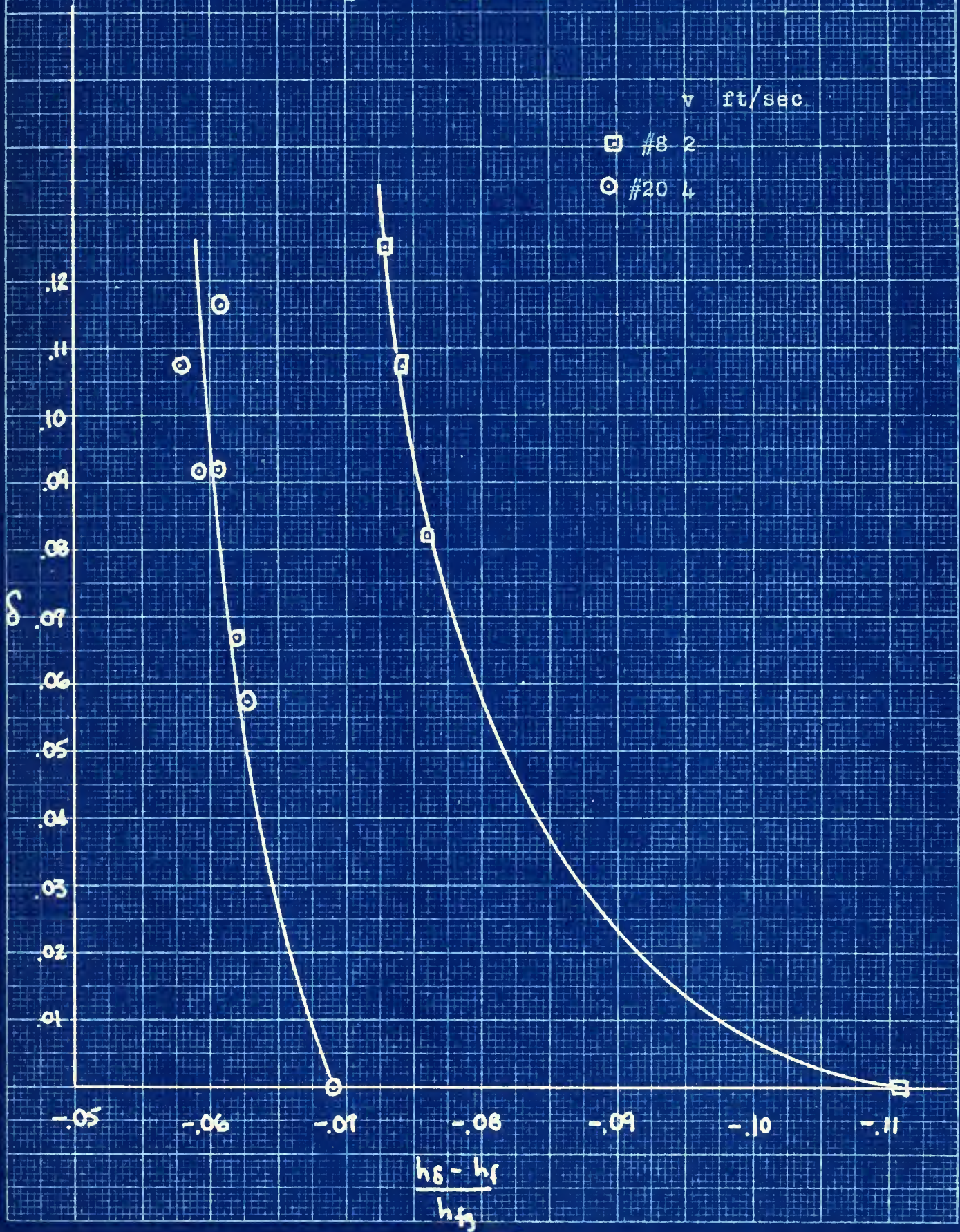

Fig. 16 - V = 1 ft/sec.

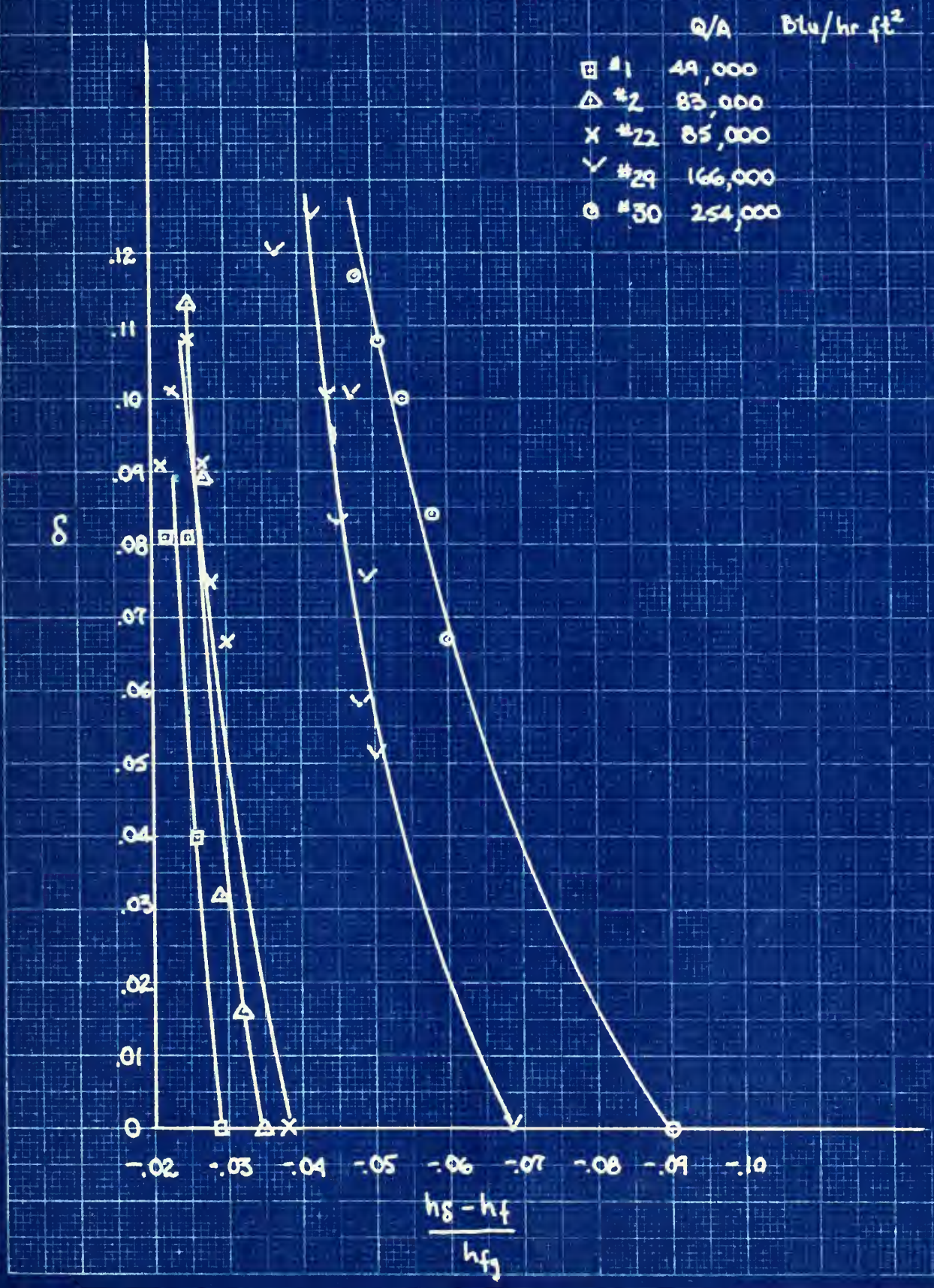

Fig. 17 - v = 2 ft/sec

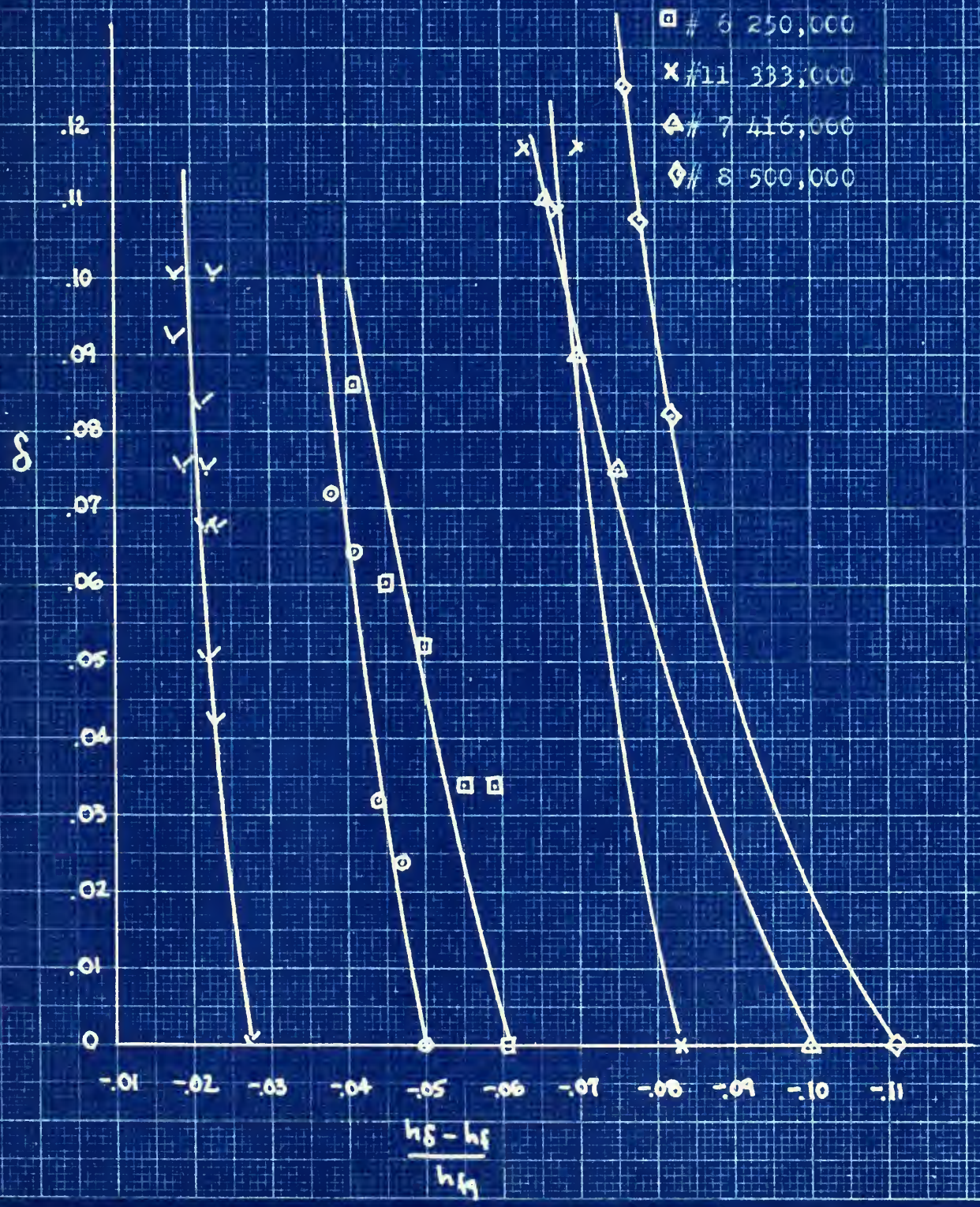

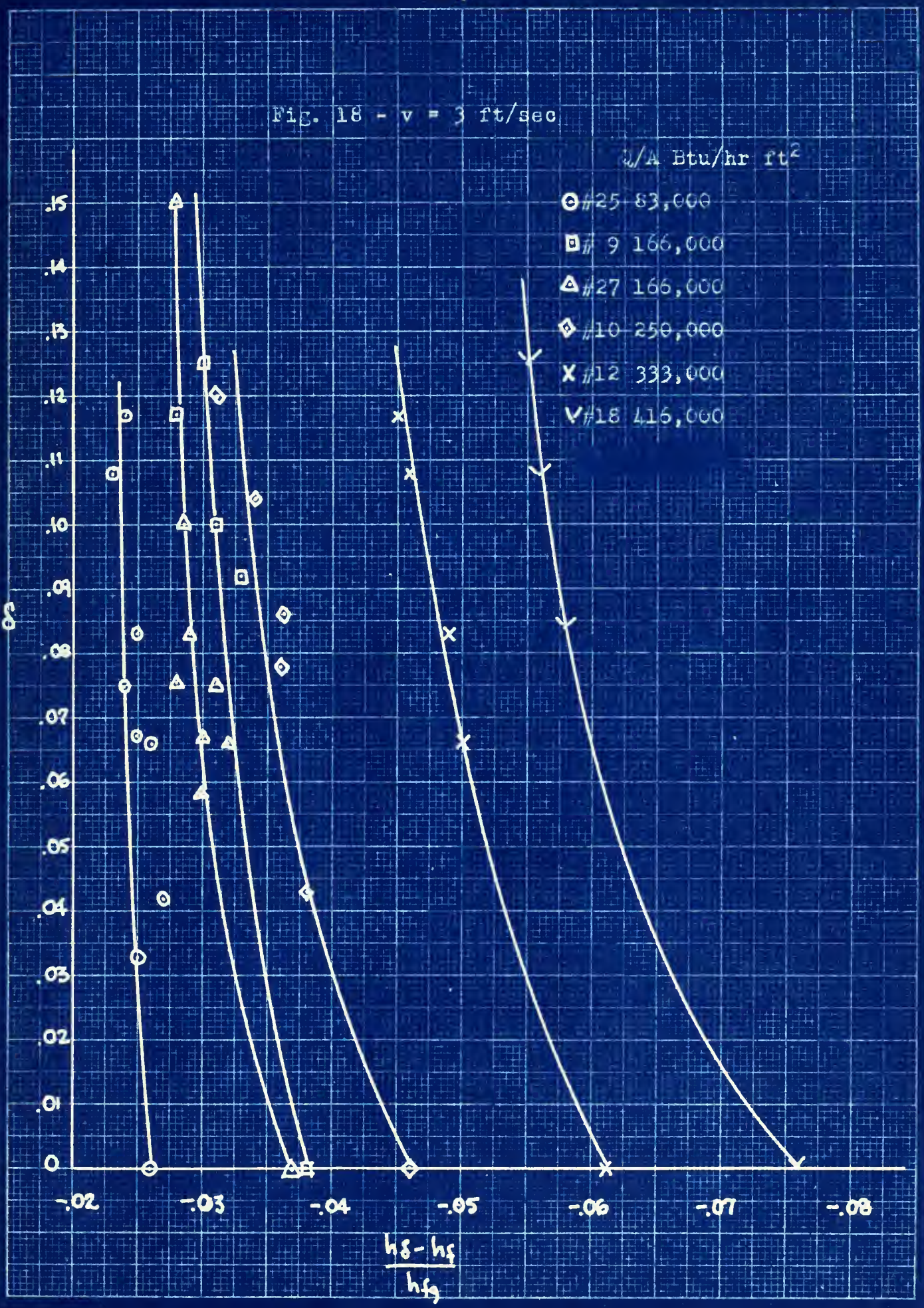

Fig. 18 - v = 3 ft/sec

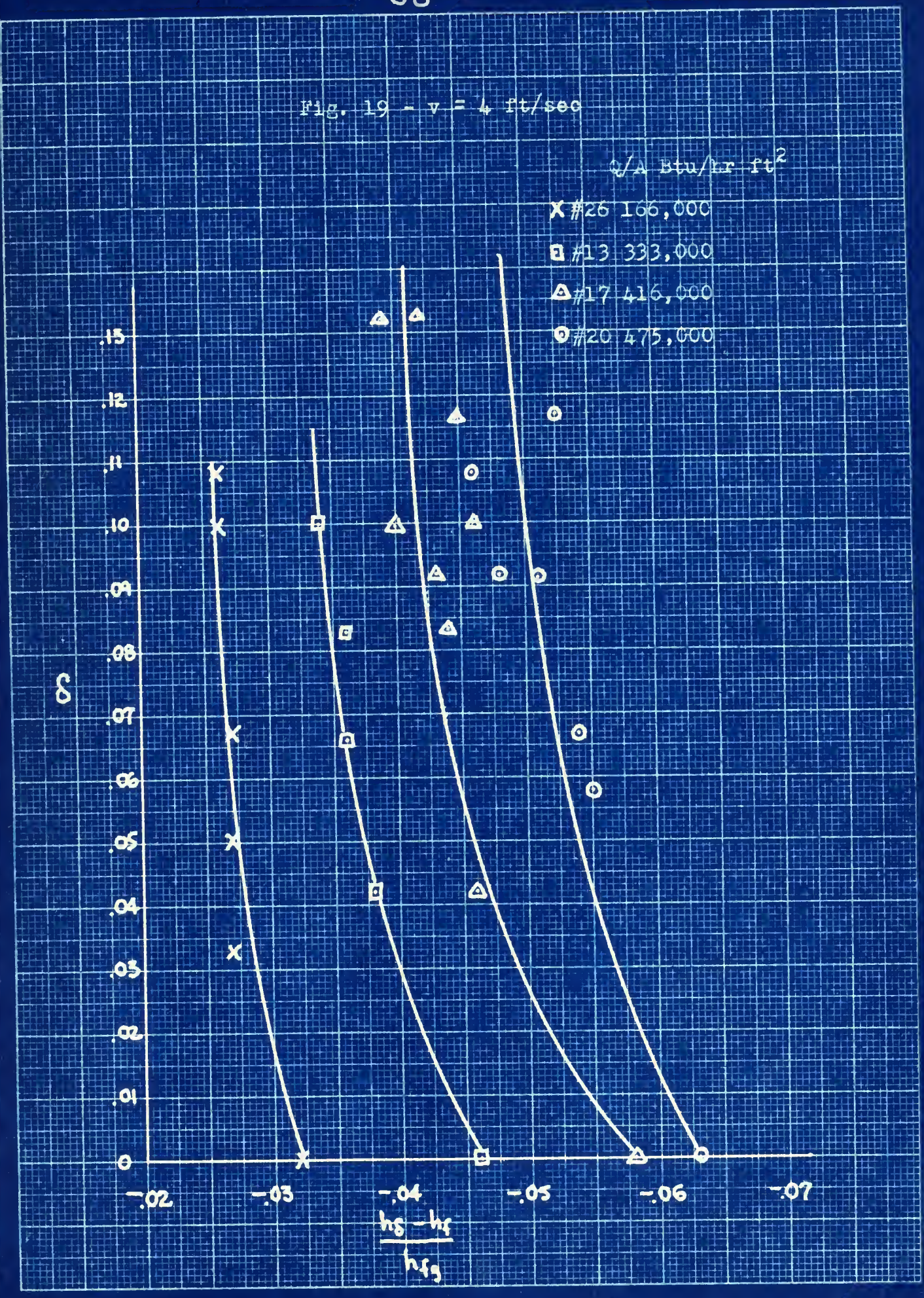
Fig. 19 - v = 4 ft/sec
Q/A Btu/hr ft²
X #26 166,000
□ #13 333,000
△ #17 416,000
⊙ #20 475,000
δ
.15
.12
.11
.10
.09
.08
.07
.06
.05
.04
.03
.02
.01
0
-.02
-.03
-.04
-.05
-.06
-.07
$\frac{h_\delta - h_f}{h_{fg}}$

Fig. 20 - v = 5 ft/sec

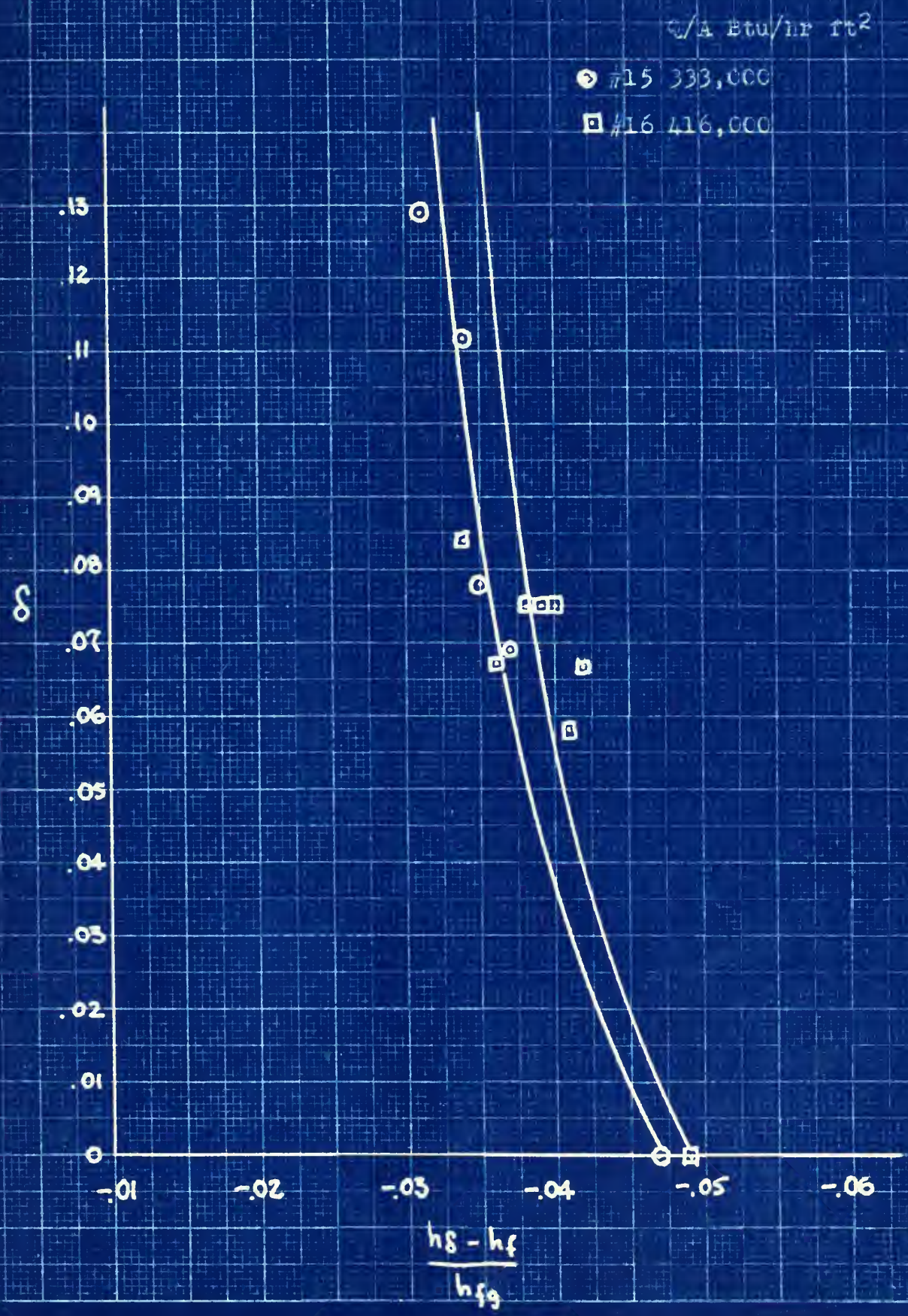

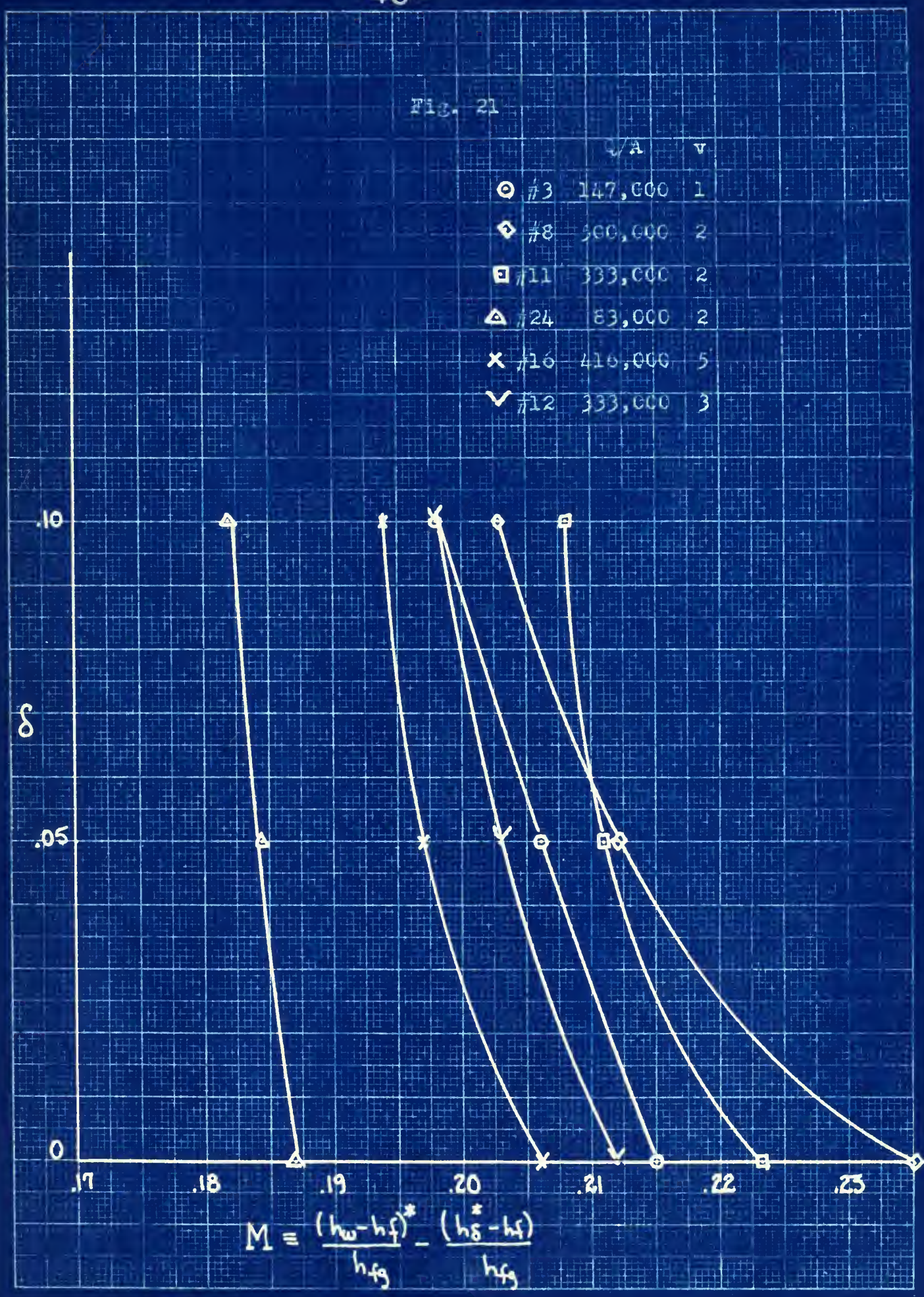
Fig. 21
Q/A
V
#3 147,000 1
#8 500,000 2
#11 333,000 2
#24 83,000 2
#16 416,000 5
#12 333,000 3
.10
.05
0
δ
.17
.18
.19
.20
.21
.22
.23
$M = \frac{(h_w - h_f)^*}{h_{fg}} - \frac{(h_\delta^* - h_f)}{h_{fg}}$

BIBLIOGRAPHY

1. Gunther, F.C., "Photographic Study of Surface - Boiling Heat Transfer to Water with Forced Convection.", Trans. ASME, 73, 115-123 (1951).

2. Untermeyer, S. "Boiling Reactors: Direct Steam Generation for Power." Nucleonics, 12, July 1954.

3. "Density Transients in Boiling Liquid Systems" Interim Report 52.17, July 1952, CLR AECU-2169 Univ. of Cal., Los Angeles, Calif.

BIBLIOGRAPHY

1. Mantner, K.C., "Photogrammetric Study of Surface - Mounting Rate Transmitter to Water with Forced Convection", Trans. AGU, 32, 113-121 (1951).

2. Waterbury, L. "Polling Equipment: Large Item Generation for Power," Instruments, 32, July 1959.

3. "Remote Transmitters in Moving Light Systems" Interim Report 56.17, July 1952, U.S. Hydrog. Univ. of Del., Los Angeles, Calif.

28871

D97 Dyer
An investigation into the growth of a boiling boundary layer in turbulent flow.

28871

D97 Dyer
An investigation into the growth of a boiling boundary layer in turbulent flow.

thesD97
An investigation into the growth of a bo
3 2768 001 89632 7
DUDLEY KNOX LIBRARY